

LLL gas stimulation program quarterly progress report October through December 1979

**M. E. Hanson, G. D. Anderson,
R. J. Shaffer, D. F. Towse,
W. Lin, L. D. Thorson, and M. P. Cleary**

February 1980



**Lawrence
Livermore
Laboratory**

This report was prepared as an account of work sponsored by the United States Government. Neither the United States nor the United States Department of Energy, nor any of their employees, nor any of their contractors, subcontractors, or their employees, makes any warranty, express or implied, or assumes any legal liability or responsibility for the accuracy, completeness or usefulness of any information, apparatus, product or process disclosed, or represents that its use would not infringe privately owned rights.

Reference to a company or product name does not imply approval or recommendation of the product by the University of California or the U.S. Department of Energy to the exclusion of others that may be suitable.

Work performed under the auspices of the U.S. Department of Energy by the Lawrence Livermore Laboratory under Contract W-7405-Eng-48.

**LLL gas stimulation program
quarterly progress report
October through December 1979**

**M. E. Hanson, G. D. Anderson,
R. J. Shaffer, D. F. Towse,
W. Lin, L. D. Thorson, and M. P. Cleary***

Manuscript date: February 1980

*Massachusetts Institute of Technology

LAWRENCE LIVERMORE LABORATORY 
University of California • Livermore, California • 94550

PREFACE

Although U.S. gas resources remain large, proven reserves have declined to 230 trillion feet, and the current reserves/production ratio is 10 to 1.

It is estimated that tight (i.e., low-permeability) western gas reservoirs and eastern Devonian gas shales contain large quantities of natural gas, but because of the low permeability, these resources have been difficult to recover. Some gas has been produced, but industry needs more economical recovery techniques. The region around the production wells must be stimulated in some manner to induce a more rapid flow into the well bore. The stimulation process involves creating channels or cracks out into the reservoir from the well bore. This can be done by detonating high explosives or nuclear explosives in the well bore or by hydraulically fracturing the formation.

Currently, the most promising techniques for stimulating low-permeability gas reservoirs are hydraulic fracturing and massive hydraulic fracturing (MHF). Hydraulic fracturing involves pumping fluids under high pressure down the well bore and out into the reservoir. The hydraulic action fractures the rock around the well bore, and proppants in the fracturing fluids hold the cracks open. The fractures provide large drainage faces for the gas and channel it into the well bore. Hydraulic fracturing has been routinely used in oil-well completion and cleanup for many years. MHF differs from hydraulic fracturing in that larger amounts of fluid and proppant are pumped down the well to create and prop fractures at much greater distances.

The application of MHF techniques to tight western gas formations has given variable and sometimes disappointing results. The best efforts of a CER-led industry/government consortium to stimulate the Piceance Basin near Rio Blanco, Colorado, were not successful. On the other hand, Amoco has used MHF techniques in the Wattenburg field near Denver with a high degree of success. Significant differences in the reservoirs themselves apparently account for the differences in success.

The Devonian shales present similar problems. It is believed that production from these gas shales results from the connection of the wells to the existing fracture patterns. Hence, to recover this gas, we must locate the producing zones, locate the natural fractures near the well bore, and fracture from the well bore to the existing fractures.

The Lawrence Livermore Laboratory (LLL) has embarked on a research program to help develop tight gas reservoirs in the United States. We are trying to obtain a more detailed understanding of the stimulation processes, including how the formation properties interact with and affect these processes. The problem is to determine how to connect the maximum amount of productive reservoir rock to the well bore through a highly permeable fracture system.

There are several questions that we would like to be able to answer in advance about the tight Rocky Mountain formations. Can we identify particular sections where the fractures may be expected to be preferentially confined to the productive sands, so that a maximum volume of reservoir can be stimulated? What is the geometry (length, width, and number) of the fractures? What is the nature of the treatment (fluid composition, volumes, pumping rates, perforation intervals) which, when applied to a formation with certain properties, will result in optimum and economical recovery? What are some of the important geophysical measurements and experiments that can aid in this endeavor? What data and experiences exist that are relevant? Most of the western reservoirs contain a high degree of water saturation, which can significantly reduce the already low permeability of these reservoirs; is it possible to use existing logging techniques supplemented by new geophysical measurements to ascertain the *in situ* water saturation?

Devonian shales present many of the same challenges as the tight Rocky Mountain formations. There are, however, some special problems. Logging techniques for these shales are just being developed, and we have not yet acquired the ability to locate the fractures that do not intersect the well bore. The effect of hydraulic fracturing on Devonian shales is also not well understood. Water, one of the standard hydraulic fracturing fluids, can cause significant formation damage; organic and cryogenic fluids are expensive; high-explosive fracturing makes well clean-out and completion costly and uncertain; and, as we have shown previously,¹ the diameter of permeability enhancement is small.

Our program is primarily investigative. We are not currently proposing any field programs. We are, however, constructing and applying theoretical models and performing laboratory experiments to develop an

understanding of the gas stimulation process. These tasks are complementary, and parallel development is necessary. Another facet of the program is geophysical measurement (logging) in the environments where these stimulation processes are applied. Close association with the DOE-supported field programs provides the interaction and direction necessary to the program.

The LLL program can be broken into eight task areas: (1) theoretical modeling of the hydraulic fracturing process; (2) laboratory hydraulic fracturing experiments; (3) log tool development and analysis of log data; (4) cataloging and evaluation of pertinent geological and geophysical reservoir data; (5) measurement of pertinent reservoir properties; (6) reservoir analysis; (7) evaluation of other stimulation techniques; and (8) environmental reports in support of DOE field programs.

CONTENTS

Preface	iii
Abstract	1
Theoretical Analysis	2
Crack Growth Near Frictional Interfaces	2
Dynamic Fracture Propagation Near Interfaces	5
Fluid Flow in an Expanding Crack	6
Fluid Front Advancement in Stationary Cracks	8
Experimental	18
Frictional Threshold Experiments	18
Fluid Flow Experiments	18
Geology and Geophysics	21
Development of Tight Western Gas Sands	21
Introduction	21
Fracture Literature	21
Tight Gas Sands	22
Stresses in Rock	22
Regional and Local Stresses	24
Factors Controlling Fractures	26
Fracture Orientation	26
Summary	28
Rock Mechanics Measurements	28
References	31
Appendix A. Annotated Bibliography with Abstracts	33

**LLL gas stimulation program
quarterly progress report
October through December 1979**

ABSTRACT

This report summarizes the research and activities of the LLL Gas Stimulation Program during the final quarter of FY 1979. We have continued our theoretical model development and application. Analyses of frictional interfaces, with similar materials on both sides of the interface, show that frictional slippage along the interface tends to draw a pressurized fracture toward the interface. Increasing friction along the interface changes the position at which the pressurized fracture is affected by the interface. The dynamic effects of propagation near a well-bonded interface between two dissimilar materials are not significantly modified by the velocity of the dynamically propagating fracture for fracture by velocities below the body wave speeds. We have shown the pressure evaluation of the fracturing fluid in a crack. One notable feature of these calculations is the rather sudden increase in fluid pressure at the fracture tip just after the fluid reaches it. Frictional interface experiments using various lubricants on the interface show distinct changes in the frictional coefficient; however, these tests indicate that the interface must support about 350 psi (24 GPa) in shear (frictional) stress before a fracture will penetrate the interface. Our studies of the occurrence and mechanics of natural fractures in the western reservoirs show that in a relaxed tectonic setting, one principal stress is most often nearly vertical and the other two are horizontal. Local stresses that control small fractures such as joints may be different from, although compatible with, the regional stresses. Fractures are controlled by the physical environment, the stresses, and changes in stresses due to burial and uplift. Jointing frequency is greater in weak and thinly bedded rocks and is directly related to the intensity of folding.

THEORETICAL ANALYSIS

CRACK GROWTH NEAR FRICTIONAL INTERFACES

The mechanisms which impede fracture propagation in a reservoir strongly influence the geometry of the created fractures. In our research to enhance the application of hydraulic fracturing, we have studied and reported on some aspects of fracture propagation near material interfaces²⁻⁴ in a reservoir. Recently we have directed our efforts toward the effects of frictional interfaces.⁵ Calculations involving pressure-driven fractures near frictional interfaces were reported previously.⁵ We have continued these analyses. The geometry of the fracture and interfaces for these calculations are shown in Fig. 1. The mechanical properties of the materials on both sides of the interface were similar; Poisson's ratio for both materials was 0.25. The effects of pore pressure changes due to leakage of the fluid into the surrounding material were ignored.

Changes in the Mode I stress intensity factor (K_I) as the fracture approaches the interface are shown in Fig. 2. In this figure we have plotted the changes in the normalized Mode I stress intensity factor (K_I)⁵ for five values of $\gamma = \tau_f/p_c$, where τ_f is the initial frictional stress and p_c is the pressure in the crack, assumed constant along the axis of the crack. The fracture tip distance from the interface, δ , has been normalized with respect to the fracture length. The five values of γ presented in Fig. 2 are $\gamma = 0.033, 0.067, 0.1, 0.133,$ and 0.167 .

Figures 3 and 4 display changes in the strain on both sides and along the interface for the five values of γ . The strains are presented in the coordinate system defined by the interface and the crack, Fig. 1. The ordinate of these plots is parallel to the frictional interface and the abscissa is parallel to the crack. The strain values were portrayed as a function of η where $\eta = y/2c$ where c is the half crack length, with $\eta = 0$ on a line extended from the crack axis. The values of the strain are displayed for the crack tip at $\delta = 0.188$. Strains obviously vary as the fracture approaches the interface. Figure 3 shows the strains just to the left and parallel to

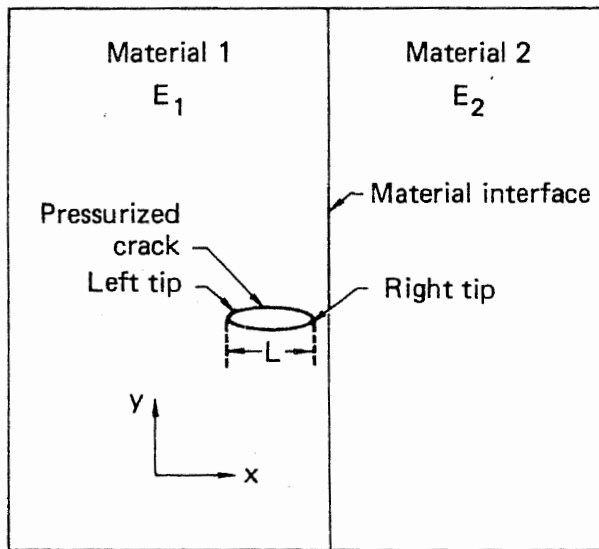


FIG. 1. Geometry of fracture near frictional interface. Note: Materials were the same in these calculations.

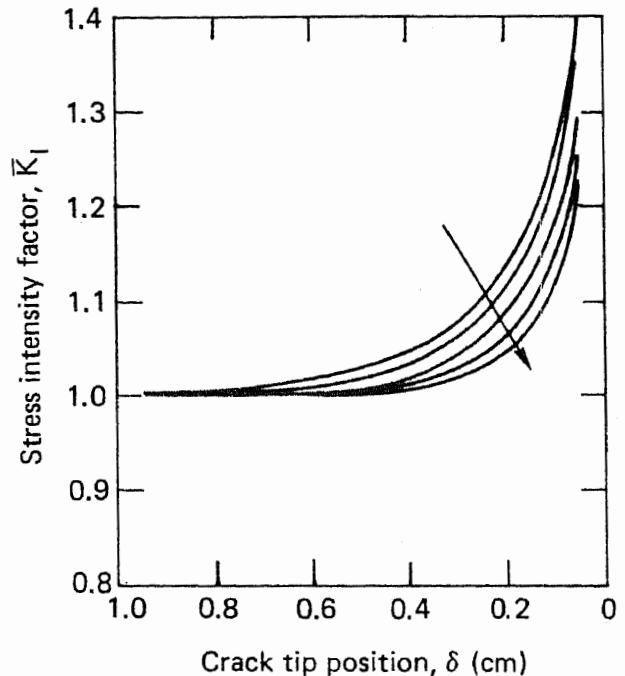


FIG. 2. Normalized Mode I stress intensity factor vs normalized distance of crack tip from interface for five values of initial frictional stress along interface (γ is ratio of initial frictional stress along interface to pressure in crack—see text).

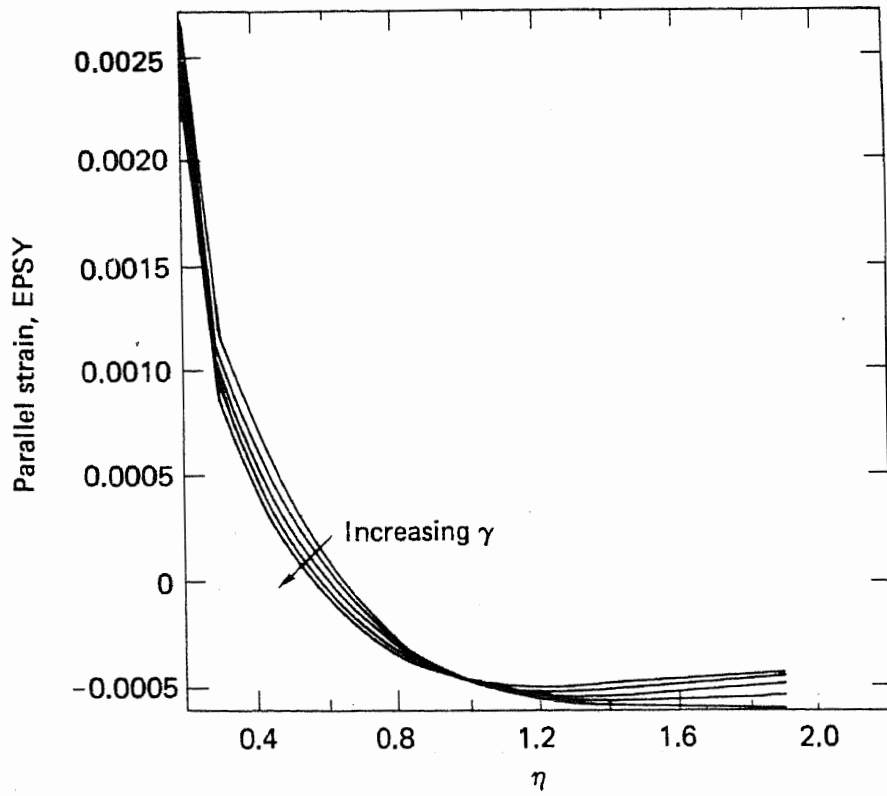
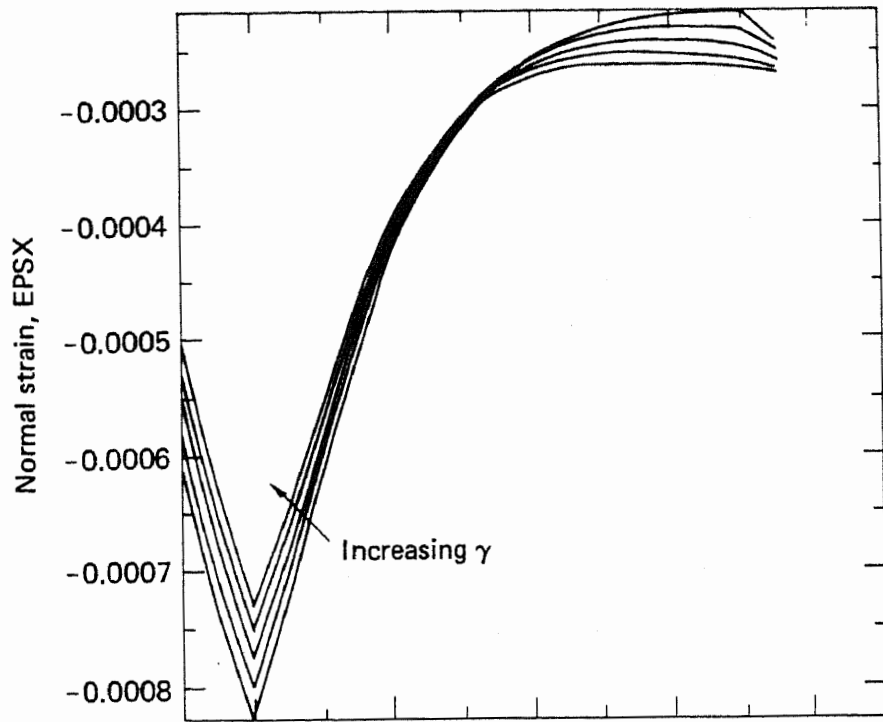


FIG. 3. Normal strain, $EPSX$, and parallel strain, $EPSY$, to left of interface for crack tip position $\delta = 0.188$ (values of strain are shown for five values of interface friction; note η is 0 on crack axis and increases upward—see Fig. 1).

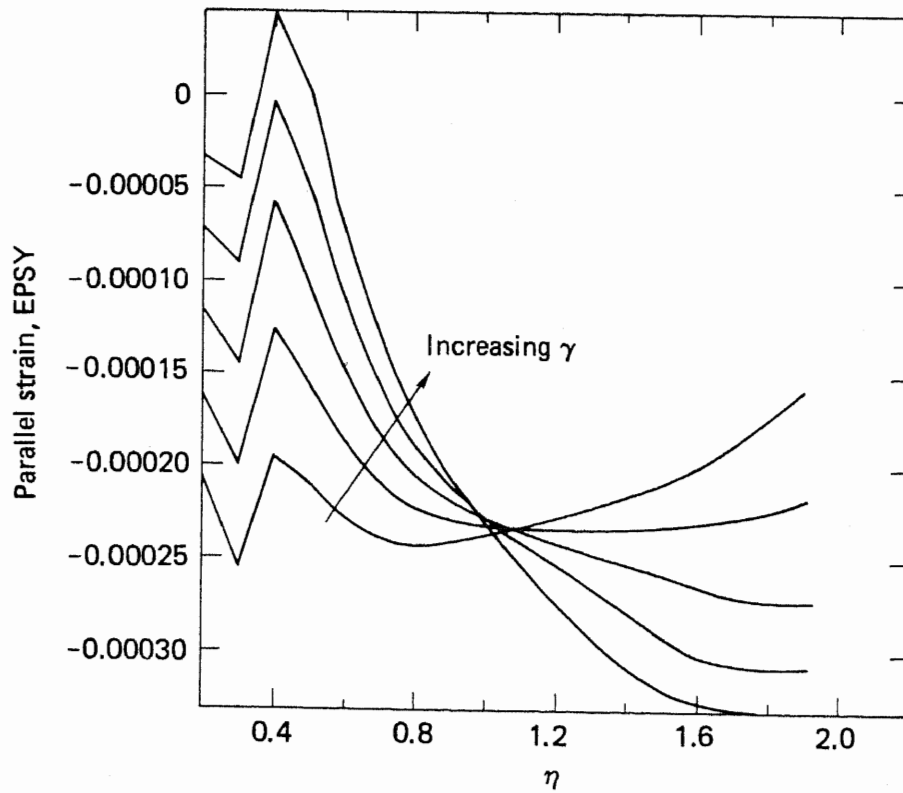
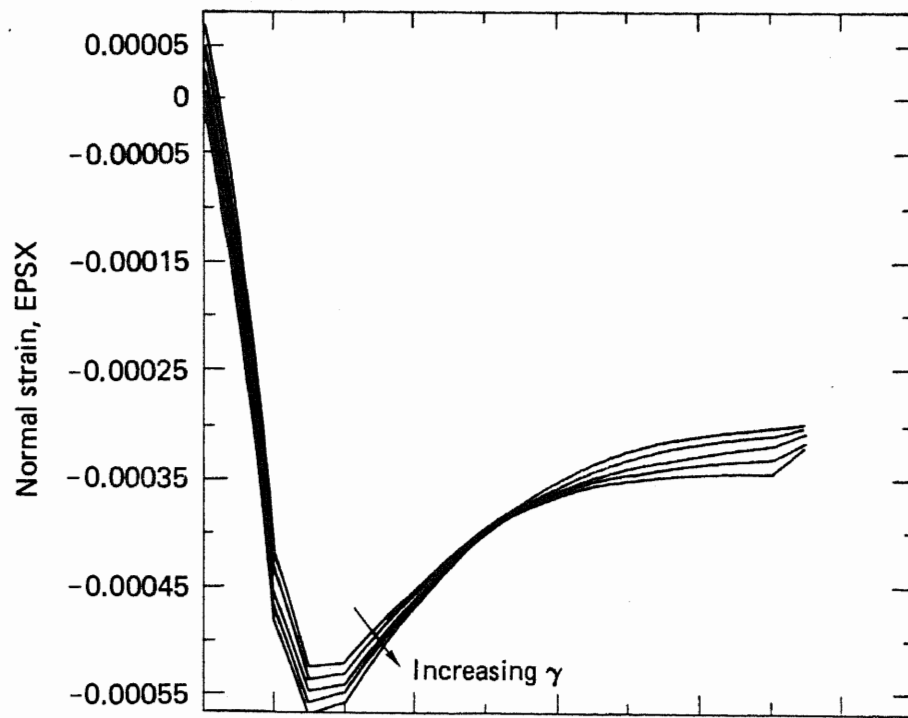


FIG. 4. Normal strain, EPSX, and parallel strain, EPSY, to right of interface for crack tip position $\delta = 0.188$ (values of strain are shown for five values of interface friction; note η is θ on crack axis and increases upward—see Fig. 1).

the interface; Fig. 4 displays the values to the right of the frictional interface. The effects of changes in friction are clearly seen by comparing the strain in the y-direction; i.e., perpendicular to the crack. It is obvious that the strain has been modified significantly by frictional slippage. The x-components of strain also display an important aspect of the fracturing process. These are manifested near the tip of the crack by a suction-like or pulling tendency. That is, material directly ahead of the crack tip is drawn toward the tip. This alters the frictional stress along the interface since the frictional stress is a linear function of the normal stress. Hence, as the fracture tip nears the interface, both normal and frictional stresses are reduced. These phenomena contribute to the rapid increase in the Mode I stress intensity factor as the fracture approaches the interface.

DYNAMIC FRACTURE PROPAGATION NEAR INTERFACES

We have previously applied our two-dimensional, time-dependent, finite-element model⁵ to determine the material overshoot characteristics caused by a pressurized crack. Such cracks initiate and propagate bilaterally at half the dilatational wave speed and stop when one tip reaches a well bonded interface. The geometry is shown in Fig. 5. The densities of both materials were 2.7 g/cm^3 . We made three calculations, corresponding to three sets of values for the Lamé elastic constants of the second material: 10, 30, and 90 GPa. These elastic constants for the first material were 30 GPa; they remained unchanged for the three calculations. A change in elastic constants at the interface results in an impedance mismatch at the interface. The impedance mismatch affects elastic wave transmission and reflection. We found that the perpendicular displacement of a point near the interface was strongly dependent on the elastic constants. Maximum displacement occurred when the first material was the stiffer of the two. For each calculation, maximum displacement occurred just before $3 t_b$, where t_b is the time elapsed from crack initiation to stopping.

In the previous calculations the crack was made to propagate at half the dilatational wave speed. We wanted to know how dependent the overshoot phenomenon was on this crack velocity. Consequently, we performed similar calculations at a significantly lower crack velocity: three-tenths of the dilatational wave speed.

The results of these calculations are shown in Fig. 6. When compared to the previous calculations⁵ we find that the character of the curves remained similar but the curves were condensed somewhat in time. The maximum displacements occur at about $2 t_b$ for the slower crack velocity. We conclude that the crack extension characteristics are relatively independent of crack velocity when the velocity is in the range of the shear wave speed. We do note, however, that the presence of material overshoot would tend to assist interface penetration.

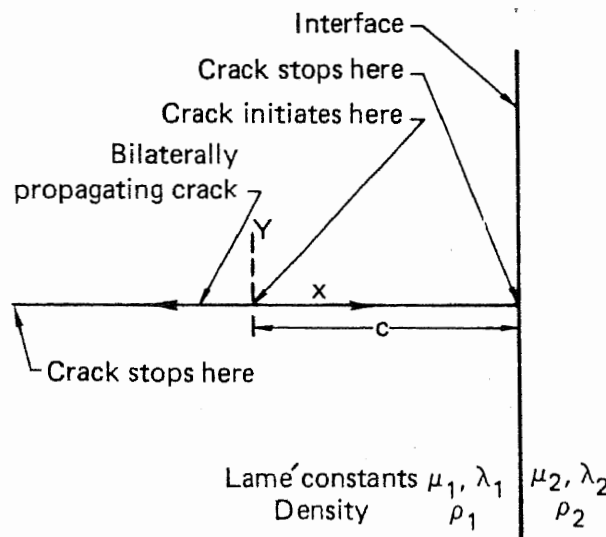


FIG. 5. Geometry of time-dependent crack problem.

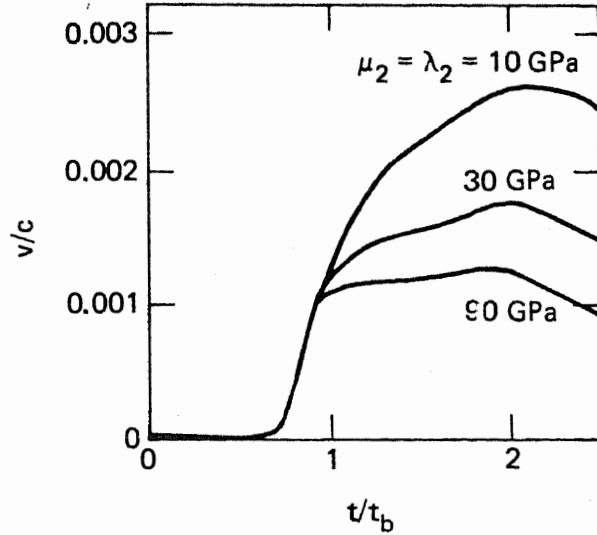


FIG. 6. Displacement of point $x = 0.8 c$, $y = 0.1 c$ in y direction when crack speed is three-tenths of dilatational wave speed (elastic constants for material 1 are 30 GPa each so that center curve corresponds to homogeneous case).

FLUID FLOW IN AN EXPANDING CRACK

We are currently developing a model to calculate the fluid flow in a propagating crack. Numerical techniques are being pursued to solve the equations for conservation of mass and momentum.

At present we assume that the fluid is incompressible and isothermal, and that the problem is two-dimensional. The equations are expressed in terms of the primitive variables u , v , p . The equations to be solved are then written as

$$\frac{\partial u}{\partial x} + \frac{\partial v}{\partial y} = 0, \quad (1)$$

$$\frac{\partial u}{\partial t} + \frac{\partial(u^2)}{\partial x} + \frac{\partial}{\partial y}(uv) = -\frac{\partial P}{\partial x} + \frac{1}{\text{Re}} \left(\frac{\partial^2 u}{\partial x^2} + \frac{\partial^2 u}{\partial y^2} \right), \quad (2)$$

$$\frac{\partial v}{\partial t} + \frac{\partial(uv)}{\partial x} + \frac{\partial(v^2)}{\partial y} = -\frac{\partial P}{\partial y} + \frac{1}{\text{Re}} \left(\frac{\partial^2 v}{\partial x^2} + \frac{\partial^2 v}{\partial y^2} \right), \quad (3)$$

where u and v are the velocities in the x and y directions respectively, Re is the Reynolds number equaling $\rho_0 v_0 L / \mu_0$, ρ_0 is the reference density, v_0 is a reference velocity, L is a reference length, μ_0 is a reference viscosity, and P is the pressure.

The boundary conditions on the walls are written for the tangential and normal velocities, respectively, as

$$u_t = 0 \quad (4)$$

$$u_n = u_n + \frac{k}{\mu} \frac{\partial P}{\partial n} \quad (5)$$

The normal velocity includes the component of flow out of the crack since the surrounding rock is assumed permeable.

This system of equations will be solved using finite differences in a way that closely follows the MAC⁶ (marker and cell) method without the use of marker particles. This method has been used with good results for a number of years. It uses a forward-time, centered-space differencing scheme. For stability reasons the pressure is zone-centered and the velocities are defined on the cell boundaries.

One additional equation is needed to relate pressure with known quantities. To do this a Poisson's equation for pressure is developed from Eqs. (1) through (3). Equation (2) is differentiated with respect to x and Eq. (3) with respect to y . The two are then added. Using continuity, Eq. (1), the final result can be written as

$$\nabla^2 P = -\frac{\partial^2(u^2)}{\partial x^2} - 2\frac{\partial^2(uv)}{\partial x\partial y} - \frac{\partial^2(v^2)}{\partial y^2} - \frac{\partial D}{\partial t} + \frac{1}{\text{Re}}\left(\frac{\partial^2 D}{\partial x^2} + \frac{\partial^2 D}{\partial y^2}\right), \quad (6)$$

where the dilatation term D is defined as

$$D = \frac{\partial u}{\partial x} + \frac{\partial v}{\partial y}. \quad (7)$$

This is recognized as a continuing equation which should be zero. However, each time-step has a small error in the velocity calculation which makes a non-zero. The dilatation term then serves as a correction factor for the next time-step and must, therefore, be retained.

Each cycle in the calculation will consist of the following steps. First, the pressure distribution will be found using Eq. (6). Next, the velocity field will be solved using Eqs. (2) and (3). Then the crack boundary will be moved to its new position. An iterative procedure will be needed to go through these steps.

How to handle the moving boundary is not clear at present. Viccelli has shown how to incorporate a moving boundary into a MAC⁷ formation but only for free slip boundaries; i.e., $u_t = 0$. Since our problem involves no-slip boundaries this method will have to be extended or a new formulation found.

At present a code to solve this problem is under development. Initially, the code will not include the moving boundary; this will be added later.

As part of the model to analyze the pressure and flow distribution in a hydraulic fracture, the fracture aperture and shape must be determined to define the boundaries of the flow regimes in the crack. The aperture and shape for a crack of length $2c$, subject to an arbitrary internal pressure distribution P_0P_1 , can be written as⁸

$$u_y(x,0) = b \int_{x/c}^1 \frac{t q_1(t) dt}{\sqrt{t^2 - x^2/c^2}}, \quad (8)$$

where

$$b = \frac{2(1 - \nu^2) p_0 c}{E}, \quad (9)$$

$$q_1(t) = \frac{2}{\pi} \int_0^t \frac{p_1(u) du}{\sqrt{t^2 - u^2}}, \quad (10)$$

where $u_y(x,0)$ is the function defining the displacement along the crack face. E is Young's modulus and ν^2 is Poisson's ratio.

The equations describing the crack aperture have been coded and debugged for solution on the computer and comparison with the analytic solution, where $P_1(x)$ is constant over the length of the crack. The analytic solution shows that the crack has an elliptical shape; e.g., $u^2/b^2 + x^2/c^2 = 1$. We have also completed a set of calculations where the pressure distribution in the crack was arbitrary and not constant over the crack surface. Others⁹ have also performed similar calculations. For these preliminary calculations, we did not include a far-field stress. Inclusion of a far-field stress is a linear superposition with the pressure in the crack.

The boundary conditions for the three problems analyzed were:

$$\begin{aligned} \sigma_{yy} &= p(x), \quad y = 0 \quad |x| < a \\ \sigma_{xy} &= 0, \quad y = 0 \\ u_y &= 0, \quad y = 0 \quad |x| > a, \end{aligned} \tag{11}$$

where a is the half crack length, σ_{yy} is the stress component normal to the two-dimensional crack axis, σ_{xy} is the shear stress, and u_y is the displacement normal to the crack axis. In defining $p(x)$ it is convenient to define a variable x_1 , which is a length bounded by a . For each pressure distribution we made four calculations, corresponding to $x_1 = a, 0.75a, 0.5a$, and $0.25a$.

Figure 7 shows a portion of the crack shape in the quadrant $x \geq 0$ and $y \geq 0$ for the pressure distributions $p(x) = p_0$ for $-x_1 \leq x \leq x_1$ and $p(x) = 0$ for $a \geq |x| \geq x_1$. In this case, when $x_1 = a$, the crack shape is elliptic and as x_1 decreases to $0.25a$ the crack shape displaces a significantly defined "hump" near the center. We also note that the aperture at the crack center decreases by a factor of about 2 when comparing the aperture for $x_1 = a$ and $x_1 = 0.25a$. Figure 8 displays the crack shape in the quadrant $x \geq 0$ and $y \geq 0$ for a parabolic distribution over a portion or all of the crack surface. Here $p(x) = p_0 \sqrt{1-|x|/x_1}$ for $-x_1 \leq x \leq x_1$ and $p(x) = 0$ for $a \geq |x| \geq x_1$. In this case we note a characteristic similar to the previous results with the "hump" at the crack center though not quite as pronounced as before. We also see a factor of 2 decrease in crack aperture when the crack is loaded over a quarter of its half length as compared to the load over the entire length. Figure 9 displays the crack shape in quadrant $x \geq 0$ and $y \geq 0$. The pressure distribution in the crack for this case was $p(x) = p_0(1-|x|/x_1)$ and $p(x) = 0$ for $a \geq |x| \geq x_1$. Here again we note a characteristic similar to the other pressure distributions except that changes of slope along the crack surface are not as pronounced.

On comparing the crack shapes for the three pressure distributions we note the crack aperture decreases from a constant-, to a parabolic-, to a triangular-pressure distribution. This is not surprising because the total load decreases in each case for a given x_1 . It is also possible that, when the pressure does not reach the crack tip, the flow characteristics of a viscous fluid are influenced by the crack shape. This could also have a significant effect on the proppant deposition in the crack. The flow in the crack will be the subject of further analyses and the model used here will provide the boundary conditions for future flow calculations.

FLUID FRONT ADVANCEMENT IN STATIONARY CRACKS

A typical fluid front advancement problem is illustrated in Fig. 10. Again we use the overall elasticity equation,* suitably nondimensionalized, as already derived in Ref. 5.

$$\dot{p}(x_0) = \int_{-l}^l \gamma_D(x_0, x) [\dot{\delta}(x) - \dot{\delta}(x_0)] dx - \dot{\delta}(x_0) [\gamma(x_0, l) - \gamma(x_0, -l)] \gamma_D \equiv -\frac{d}{dx} \gamma \tag{12a}$$

*Note that this equation also applies, remarkably, to the moving crack problem. This makes solution of the latter problem much simpler with the present formulation than with other approaches.⁶

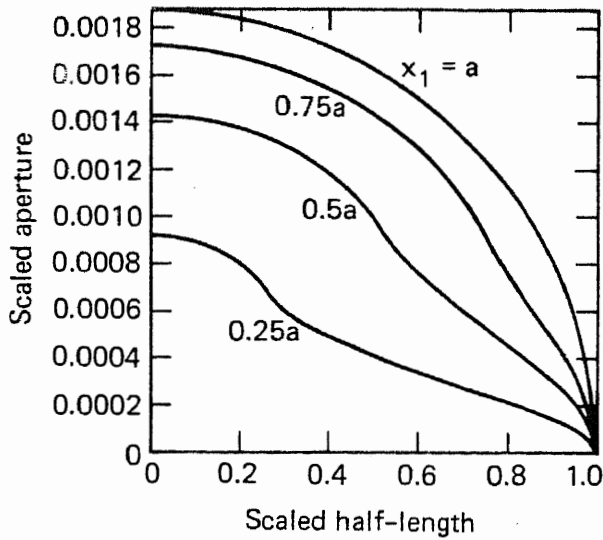


FIG. 7. Crack shape for constant pressure $p = p_0$ for $|x| \leq x_1$ and $p = 0$ elsewhere in the crack.

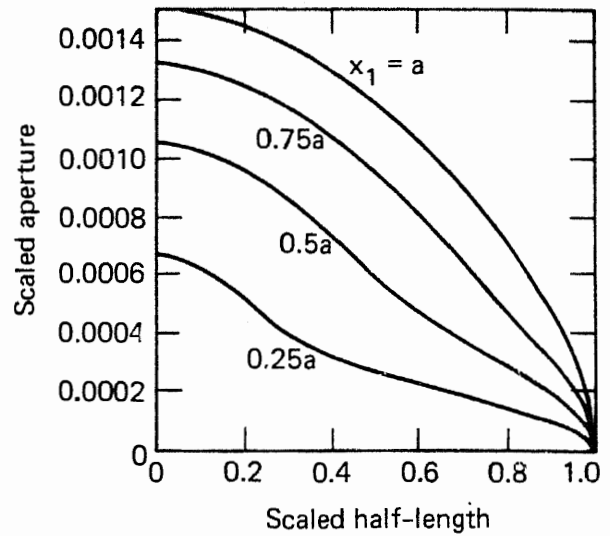


FIG. 8. Crack shape for a parabolic pressure distribution, $p = p_0 \sqrt{1-|x|/x_1}$ for $|x| \leq x_1$, and $p = 0$ elsewhere.

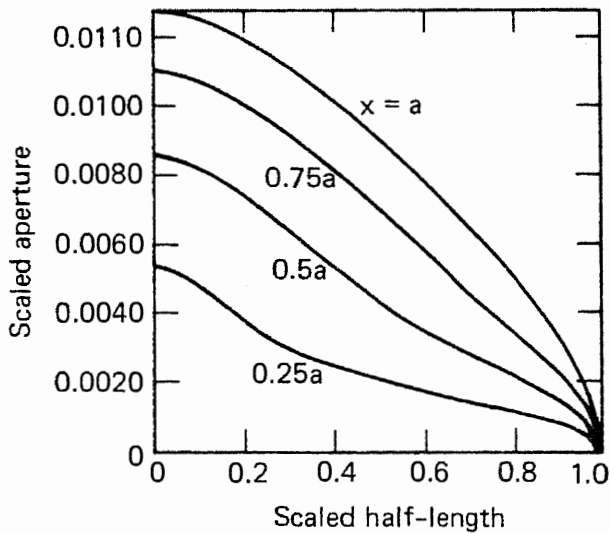


FIG. 9. Crack shape for triangular pressure distribution, $p = p_0 (1-|x|/x_1)$ for $|x| \leq x_1$, and $p = 0$ elsewhere.

NOTE

Each figure shows the crack shape for $y \geq 0$ and $x \geq 0$.

Here $\gamma(x_0, x)$ is the influence function, describing pressure P at a point x_0 on the line of the crack, due to a dislocation at point x . The latter is simply an increment of crack opening displacement δ . With reference to this equation, we may now phrase two distinct conditions. One pertains to the nonpenetrated zone (size ω) near each tip. The other prevails in the fluid-filled region (where laminar flow of Newtonian fluid has been assumed for simplicity in early testing of our routines).

$$\dot{p}(\ell \geq |x_0| \geq \ell - \omega) = 0, \quad \dot{\delta}(\ell - \omega \geq |x| \geq 0) = [\delta^3 p'] / \eta^A \quad (12b)$$

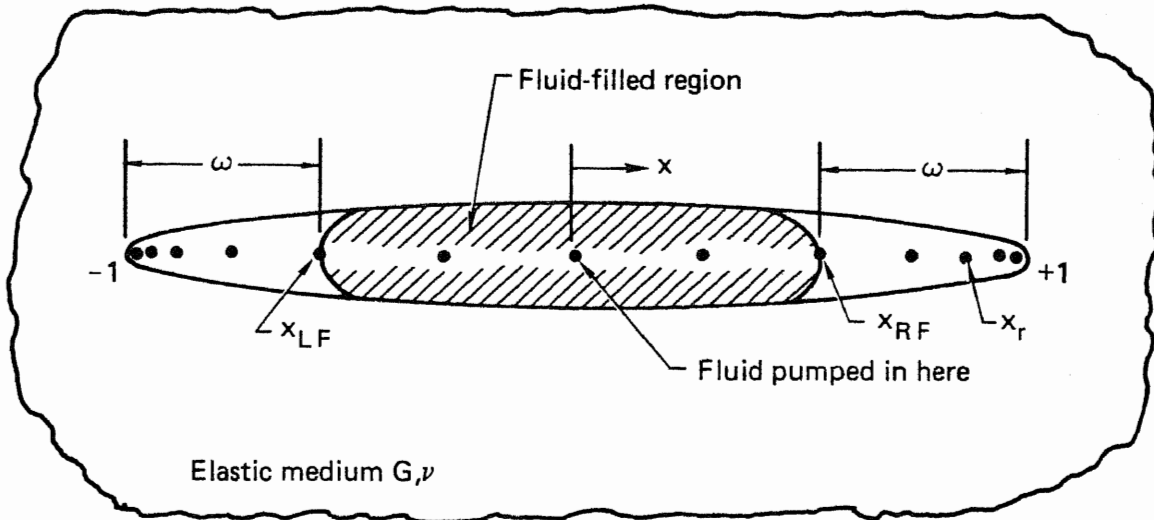


FIG. 10. Diagram of fluid front advancement problem (fluid is pumped into crack at borehole at constant pressure p_0 ; fluid front advances from one node x_r ($r = LF, RF$) to next, while crack tips are held stationary).

The fluid is assumed to have effective channel-flow viscosity $\hat{\eta}$, so that the detailed equations of fluid motion have been integrated over the channel width. We might also note that $\dot{P} = 0$, in the nonpenetrated zone, will eventually be modified to incorporate the important time-dependence caused by pore-fluid flow in the near-by vicinity.¹⁰

Thus we must solve for fluid pressure in the fluid-filled region of the crack and for crack opening rate in the empty region. Our experience with the pressure evolution problem^{5,11,12} demands that an implicit method be used for the fluid front advancement problem. Further, since we must solve for the opening rate over part of the crack, it will be convenient to construct our system of equations so as to solve for opening rate over the entire crack.

By simple approximation of time derivatives, we obtain from Eq. (12) an implicit equation for ${}^{t+\Delta t}\dot{\delta}$ and ${}^{t+\Delta t}p$ which may be written in the following numerical form⁵

$$\begin{aligned} {}^{t+\Delta t}p(x_r) - \alpha \Delta t \frac{\pi}{N} \sum_{i=1}^N \gamma_D(x_r, t_i) \left[{}^{t+\Delta t}\dot{\delta}(t_i) - {}^{t+\Delta t}\dot{\delta}(x_r) \right] \sqrt{1-t_i^2} - \alpha \Delta t {}^{t+\Delta t}\dot{\delta}(x_r) [\gamma(x_r, 1) - \gamma(x_r, -1)] \\ = {}^t p(x_r) - (1-\alpha) \Delta t \frac{\pi}{N} \sum_{i=1}^N \gamma_D(x_r, t_i) [{}^t\dot{\delta}(t_i) - {}^t\dot{\delta}(x_r)] \sqrt{1-t_i^2} + (1-\alpha) \Delta t {}^t\dot{\delta}(x_r) [\gamma(x_r, 1) - \gamma(x_r, -1)]. \end{aligned} \quad (13)$$

Over the fluid-filled region ($1 - \omega \geq |x_r, t_i| \geq 0$), this leads to the following matrix equations for the pressures at the "Chebyshev points" t_s ,

$$\begin{aligned} \sum_{\ell=1}^L \left(1 - \frac{1}{2}\delta_{\ell 1}\right) T_{\ell-1}(x_r) \sum_{s=1}^L \frac{2}{L} T_{\ell-1}(t_s) [{}^{t+\Delta t}p(t_s) - {}^t p(t_s)] = \frac{4\Delta t}{LM\tau_c} \left(\frac{\pi}{N}\right) \sum_{i=1}^N \gamma_D(x_r, t_i) \sum_{j=1}^M \{T_j'(t_i) - T_j'(x_r)\} \\ \times \sqrt{1-t_i^2} \sum_{k=1}^M T_j(t_k) \delta^3(t_k) \sum_{\ell=1}^L T_\ell'(t_s) \sum_{s=1}^L T_\ell(t_s) [\alpha {}^{t+\Delta t}p(t_s) + (1-\alpha) {}^t p(t_s)] - \frac{4\Delta t}{LM\tau_c} [\gamma(x_r, 1) - \gamma(x_r, -1)] \end{aligned}$$

$$\times \sum_{j=1}^M T_j'(x_r) \sum_{k=1}^M T_j(t_k) \delta^3(t_k) \sum_{\ell=1}^L T_\ell'(t_s) \sum_{s=1}^L T_\ell(t_s) [\alpha^{t+\Delta t} p(t_s) + (1-\alpha) t p(t_s)]; \quad t_{k,s} = -\cos \left[\frac{\pi(2(k,s)-1)}{2L} \right]$$

$$k, s = 1, \dots, L; \quad L \equiv M \equiv N+1; \quad t_i = -\cos \left[\frac{\pi(2i-1)}{2N} \right], i = 1, \dots, N; \quad x_r = -\cos(\pi r/N), r = 1, \dots, N-1. \quad (14a)$$

where $\tau_c \equiv \eta G^2/p_0^2$ is the characteristic time.¹⁰

On the other hand, $1 - \omega < |x| \leq 1$, we must use

$$\frac{L}{2} \dot{\delta}(x) = \sum_{j=1}^M \left(1 - \frac{1}{2} \delta_{j1}\right) T_{j-1}(x) \sum_{s=1}^L T_{j-1}(t_s) \dot{\delta}(t_s) \quad (14b)$$

in Eq. (13) in order to guarantee that $\dot{\delta}$ is smoothly continued from $(\delta^3 p)'$ in the penetrated region. In the non-penetrated region we must impose $\dot{p} = 0$ to allow solution for the unknown $t+\Delta t \dot{\delta}(t_s)$. Thus we solve Eq. (14a) in the penetrated region and Eq. (13) in the nonpenetrated zone, subject to the constraints

$$t+\Delta t p(t_s) = 0 \begin{cases} s = 1, \dots, LF \\ s = RF + 2, \dots, L \end{cases} \quad (15a)$$

$$t+\Delta t \dot{\delta}(1) - t+\Delta t \dot{\delta}(-1), \quad t+\Delta t p(t_{L/2}) = p_0. \quad (15b,c)$$

Note that Eqs. 15b and c are the constraints of crack closure and constant borehole pressure. Simplicity and economy may be achieved by defining the appropriate matrices*:

$$A_{r\ell} \equiv \left(1 - \frac{1}{2} \delta_{\ell 1}\right) T_{\ell-1}(x_r); \quad r = LF, \dots, RF, \quad \ell = 1, \dots, L, \quad (16a)$$

$$A'_{\ell s} \equiv \frac{2}{L} T_{\ell-1}(t_s) \quad \ell = 1, \dots, L; \quad s = 1, \dots, L, \quad (16b)$$

$$B_{ri} \equiv \frac{\pi}{N\tau_c} \gamma_D(x_r, t_i) \sqrt{1 - t_i^2} \quad r = LF, \dots, RF; \quad i = LF, \dots, RF + 1,$$

$$\equiv \frac{\pi}{N} \gamma_D(x_r, t_{i-L}) \sqrt{1 - t_{i-L}^2} \quad r = LF, \dots, RF; \quad i = L + 1, \dots, L + LF - 1$$

$$i = L + RF + 2, \dots, L + N,$$

$$\equiv \frac{\pi}{N\tau_c} \gamma_D(x_{r-L}, t_i) \sqrt{1 - t_i^2} \quad r = L + 1, \dots, L + LF - 1; \quad r = L + RF + 1, \dots, L + N - 1$$

$$i = LF, \dots, RF + 1,$$

$$\equiv \frac{\pi}{N} \gamma_D(x_{r-L}, t_{i-L}) \sqrt{1 - t_{i-L}^2} \quad r = L + 1, \dots, L + LF - 1; \quad r = RF + L + 1, \dots, L + N - 1$$

$$i = L + 1, \dots, L + LF - 1; \quad i = L + RF + 2, \dots, L + N, \quad (16c)$$

*All of the matrices are $2M \times 2M$; any undefined elements are zero.

$$\begin{aligned}
B'_{ri} &\equiv \delta_{ri} \frac{\pi}{N\tau_c} \sum_{j=1}^N \gamma_D(x_r, t_j) \sqrt{1-t_j^2} \quad r = LF, \dots, RF, \quad i = 1, \dots, N, \\
&\equiv \delta_{(r-L)i} \quad r = L + LF, \dots, L + RF, \quad i = 1, \dots, N, \\
&\equiv \delta_{ri} \frac{\pi}{N} \sum_{j=1}^N \gamma_D(x_r, t_j) \sqrt{1-t_j^2} \quad r = L+1, \dots, L+LF-1, \quad r = L+RF+1, \dots, L+N-1 \\
&\quad i = L+1, \dots, L+N, \\
&\equiv -\delta_{ri}, \quad r = L + LF, \dots, L + RF, \quad i = L+1, \dots, L+N,
\end{aligned} \tag{16d}$$

$$\begin{aligned}
C_{kj} &\equiv T'_j(t_k), \quad k = 1, \dots, M, \quad j = 1, \dots, M, \\
&\equiv \left(1 - \frac{1}{2}\delta_{j(M+1)}\right) T_{j-M-1}(t_{k-M}), \quad k = M+1, \dots, 2M, \quad j = M+1, \dots, 2M,
\end{aligned} \tag{16e}$$

$$\begin{aligned}
C'_{rj} &\equiv T'_j(x_r), \quad r = 1, \dots, N-1, \quad j = 1, \dots, M, \\
&\equiv \left(1 - \frac{1}{2}\delta_{j(M+1)}\right) T_{j-M-1}(x_{r-M}), \quad r = M+1, \dots, M+N-1, \quad j = M+1, \dots, 2M,
\end{aligned} \tag{16f}$$

$$\begin{aligned}
D_{jk} &\equiv \frac{2}{L} T_j(t_k) \quad j, k = 1, \dots, L, \\
&\equiv \frac{2}{L} T_{j-L-1}(t_{k-L}) \quad j, k = L+1, \dots, 2L.
\end{aligned} \tag{16g}$$

From here on, all undefined elements are part of a unit matrix (e.g., $E_{kl} = \delta_{kl}$), the rest being given by

$$E_{k\ell} \equiv T'_\ell(t_k) \quad k, \ell = 1, \dots, L, \tag{16h}$$

$$F_{\ell s} \equiv \frac{2}{N} T_\ell(t_s) \quad \ell, s = 1, \dots, L, \tag{16i}$$

$$\begin{aligned}
G_{rj} &\equiv \frac{\delta_{rj}}{\tau_c} [\gamma(x_r, 1) - \gamma(x_r, -1)], \quad r = LF, \dots, RF, \quad j = 1, \dots, L \\
&\equiv \delta_{rj} [\gamma(x_{r-L}, 1) - \gamma(x_{r-L}, -1)], \quad r = L+1, \dots, L+LF-1, \quad j = L+1, \dots, 2L,
\end{aligned} \tag{16j}$$

$$H_{sq} \equiv -\delta_{sq} \text{sign}(t_s) + \delta_{(L/2)s} \text{sign}(t_s) \quad s, q = 1, \dots, \ell, \tag{16k}$$

$$S_{ij} \equiv \delta_{ij} + \delta_{(M/2)j} \text{sign}(t_i) \quad i, j = 1, \dots, L, \tag{16l}$$

$$T_{jk} \equiv -\delta_{jk} \text{sign}(t_k) \quad j, k = 1, \dots, L, \tag{16m}$$

$$\Delta_{jk} \equiv \delta_{jk} \delta^3(t_j) \quad j, k = 1, \dots, L. \tag{16n}$$

Use of the following secondary matrices lends further simplification:

$$\mathbf{M1} \equiv \mathbf{DS}, \quad \mathbf{M2} \equiv \mathbf{TEFH}, \quad \mathbf{M3} \equiv \mathbf{C'DS}, \quad \mathbf{M4} \equiv \mathbf{AA'}, \quad \mathbf{M5} \equiv \mathbf{BC - B'C'}, \quad \mathbf{M6} \equiv \mathbf{TC'FH} \quad (17)$$

Now $\mathbf{M1}$, $\mathbf{M2}$, $\mathbf{M3}$, and $\mathbf{M6}$ need be computed only once; only $\mathbf{M4}$ and $\mathbf{M5}$ are time-dependent. The resulting system of equations is:

$$\begin{aligned} & \{ \mathbf{M4} - \alpha \Delta t \mathbf{M5} \mathbf{M1} \Delta \mathbf{M2} + \alpha \Delta t \mathbf{G} \mathbf{M3} \Delta \mathbf{M2} \}^{t+\Delta t} \mathbf{U} \\ & = \{ \mathbf{M4} - (1 - \alpha) \Delta t \mathbf{M5} \mathbf{M1} \Delta \mathbf{M2} + (1 - \alpha) \Delta t \mathbf{G} \mathbf{M3} \Delta \mathbf{M2} \}^t \mathbf{U} \end{aligned} \quad (18a)$$

or

$$\mathbf{M}^{t+\Delta t} \mathbf{U} = \mathbf{R}, \quad (18b)$$

where the vector of unknown variables is

$$\begin{aligned} U_s & \equiv p(t_s), \quad s = 1, \dots, M \\ \dot{\delta}(t_{s-M}) & , \quad s = M + 1, \dots, 2M \end{aligned} \quad (18c)$$

The constraints (Eq. 15) are imposed as follows: Eq. (15a) by setting $\mathbf{M}_{sj} = \delta_{sj}$, $\mathbf{R}_s = 0$ for $s = 1, \dots, \mathbf{LF}-1$, $s = \mathbf{RF} + 3, \dots, \mathbf{L}$ and $j = 1, \dots, 2\mathbf{L}$; Eq. (15b) by setting $\mathbf{B}(\mathbf{N}, 1) = 1$ and $\mathbf{B}(\mathbf{N}, \mathbf{L}) = -1$ before computing $\mathbf{M5}$, and Eq. (15c) by setting $\mathbf{M}_{L/2j} = \delta_{L/2j}$, $j = 1, \dots, 2\mathbf{L}$. The time step size (Δt) is computed, based on the velocity of the fluid front, so as to bring the front to the next node x_r at $t = t + \Delta t$. Thus, we employ

$$\frac{\Delta t}{\tau_c} = \frac{[\delta^2 p'](x_{R1})}{x_{RF+1} - x_{RF}} \quad (19)$$

Typical results for the fluid front advancement problem are shown in Figs. 11(a) through 11(t) and Table 1. The fluid was allowed to advance to the crack tips and fill the crack entirely. The pressure was then allowed to build up for a period of time afterward. The pressure distribution behaved as one might expect: the curves became steeper near the tips as time progressed and the crack filled out very quickly. One notable feature was the rather sudden increase in the fluid pressure at the tip just after the fluid reached it—Figs. 11(e) and 11(f).

The curves showing the crack opening rate—Figs. 11(n) through 11(t)—undergo a change of character between the initial step—Fig. 11(n)—and the final step—Fig. 11(t). Before the fluid front reached the tip—Fig. 11(q)—, δ showed high narrow peaks near, but somewhat behind, the points corresponding to the location of the fluid fronts. This phenomenon seems to be consistent with the large pressure gradient that developed at the fluid fronts. After the fluid filled the crack, the peaks broadened and the overall magnitude began to decline—Figs. 11(r) through 11(t). The shape of the initial curve—Fig. 11(n)—is not unlike that of the final curve, although the initial curve has a much smaller magnitude.

The velocity of the fluid front is compared to the velocity of the same fluid flowing between two parallel plates, with a space of δ ($t: x = 0$) between them and being driven by a uniform pressure gradient of $p'/p_0 = 1.0$ (Fig. 12). This velocity is also calculated by Eq. (19). Initially there is a large discrepancy between this latter velocity (dashed curve) and the calculated fluid front velocity. This result is consistent with the difference between the crack opening at the fluid front (0.4) and the maximum opening (1.0). As time progresses,

TABLE 1. Parameters for which pressure evolution, opening displacement, and opening displacement rate are presented in Fig. 11.

t/τ_c	x_{RF}	$\Delta t/\tau_c$
0	0.6802	0.8224
0.8224	.7818	.1418
0.9705	.8660	.09725
1.068	.9309	.03118
>1.168	0.9972	0.03118

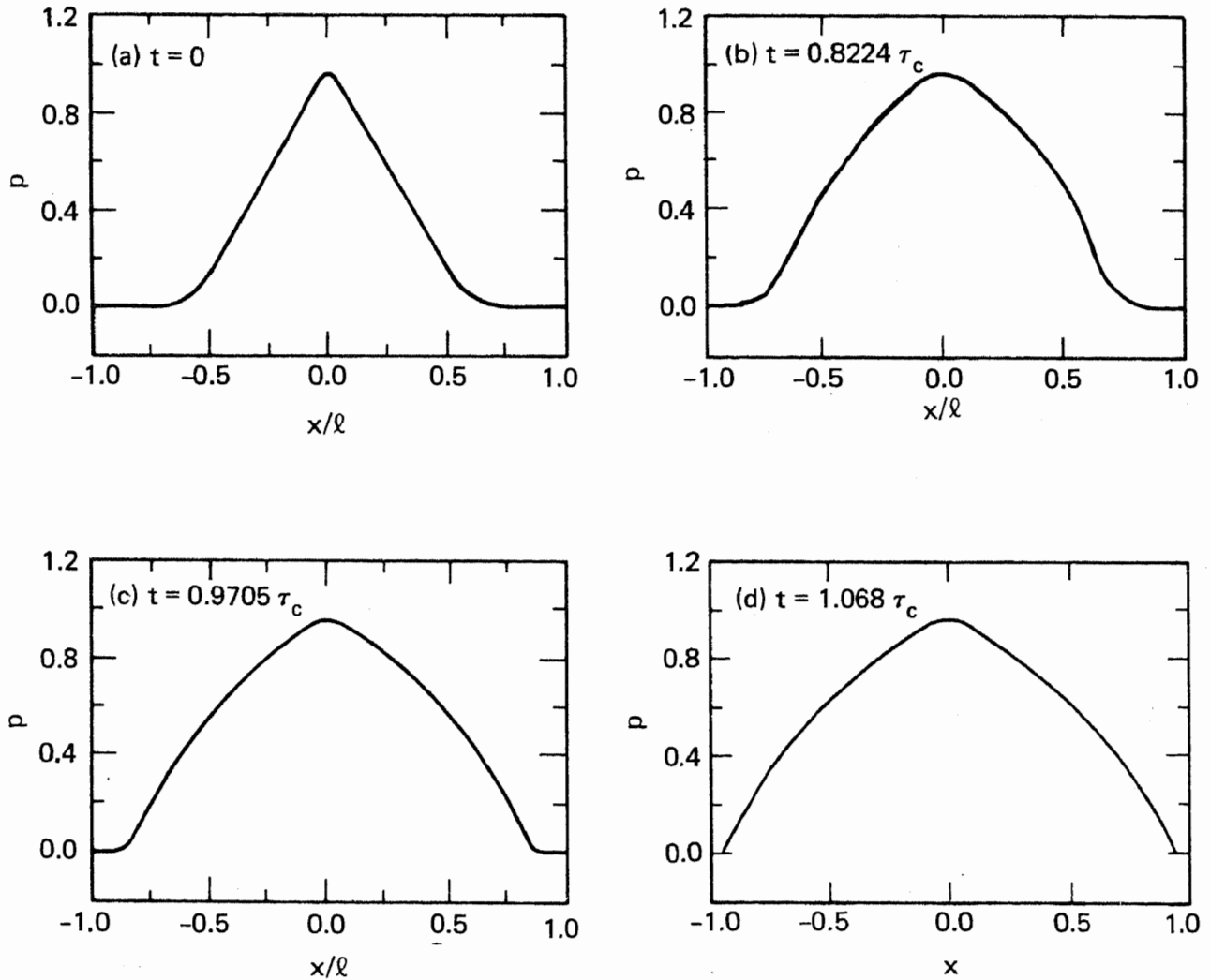


FIG. 11. Curves showing fluid front advancement and pressure evolution in a stationary crack (note rapid change in pressure distribution when fluid reaches crack tips (e), (f) and changes in shape of opening rate (δ) curves as crack is being filled; (a)-(g) p ; (h)-(m) δ ; (n)-(t) $\dot{\delta}$; here we have used $p_0/G = 1$, $\hat{\eta}/G = 1$, $\nu = 0.3$).

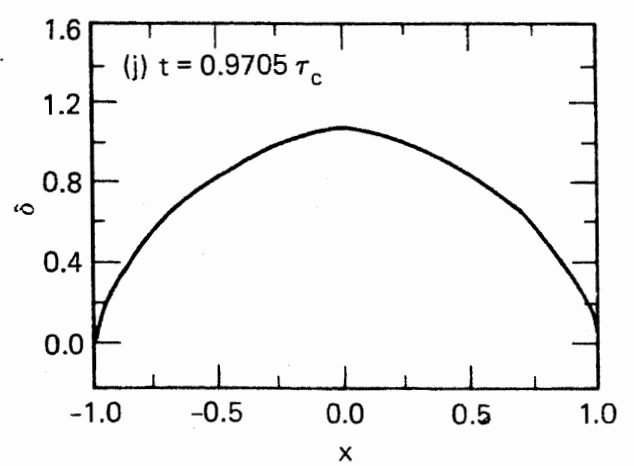
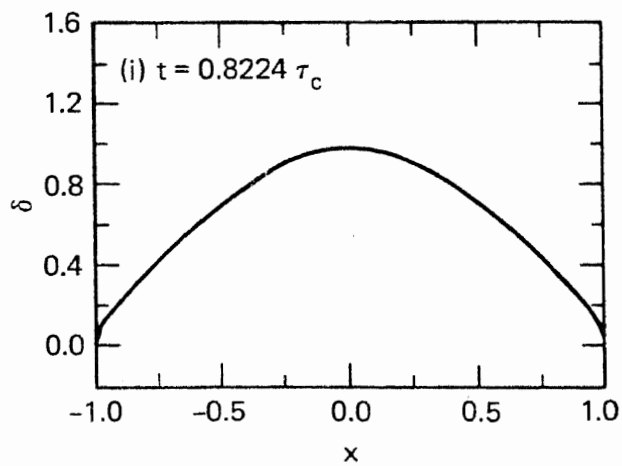
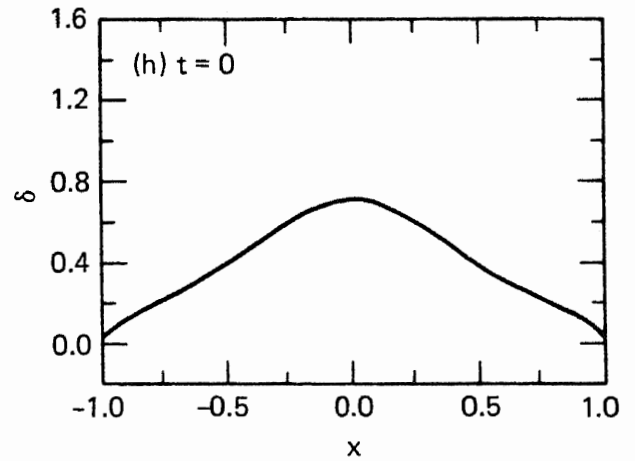
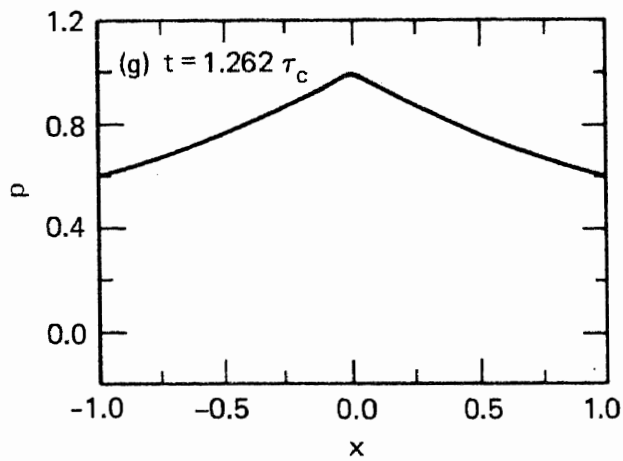
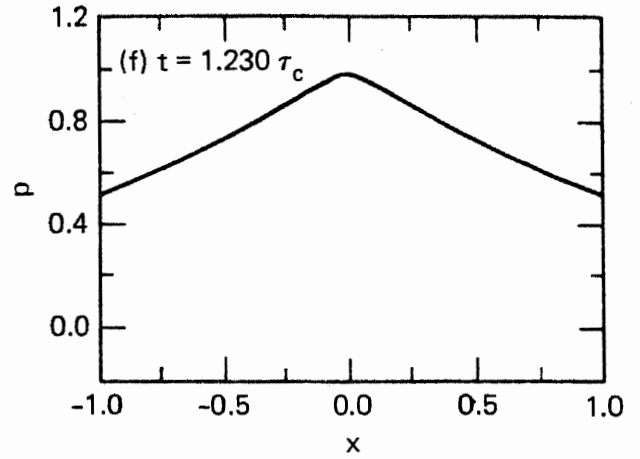
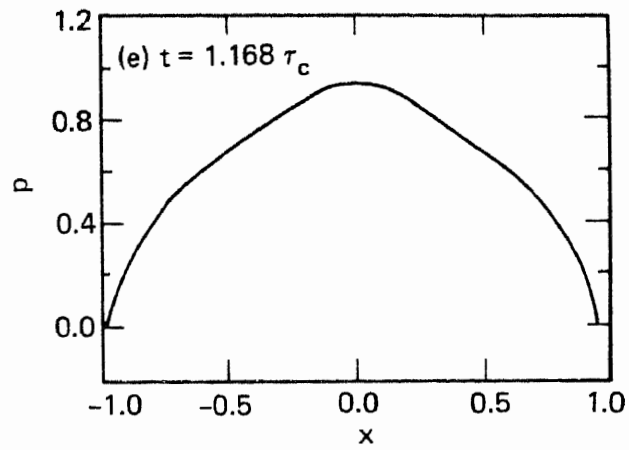


FIG. 11. Continued.

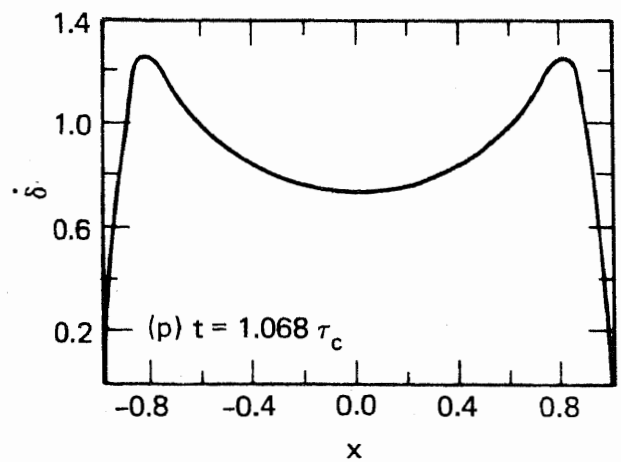
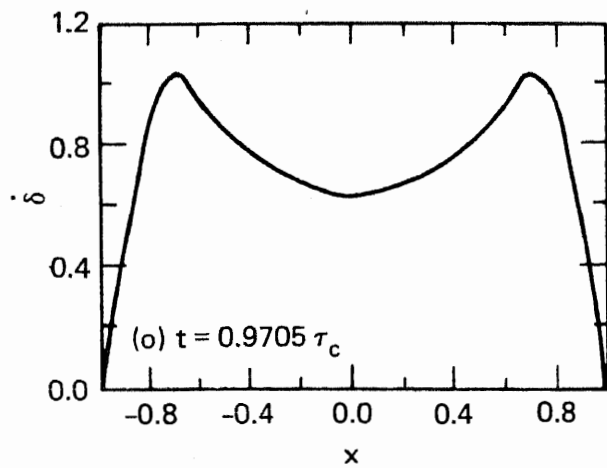
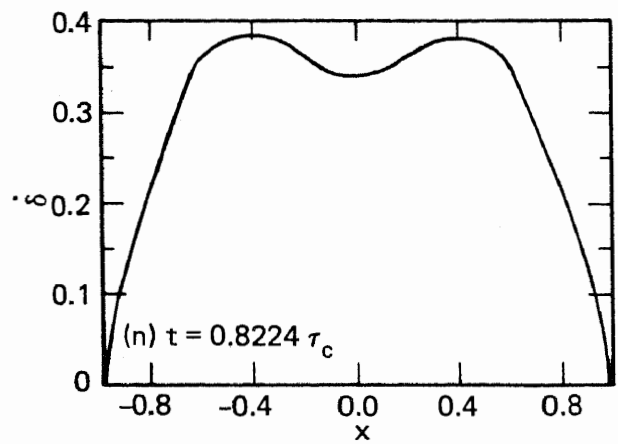
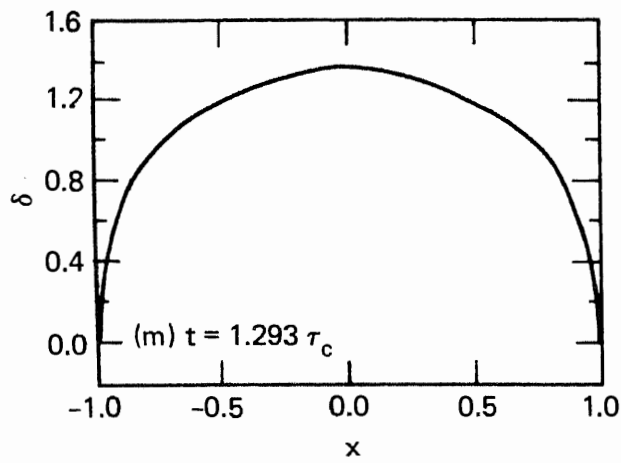
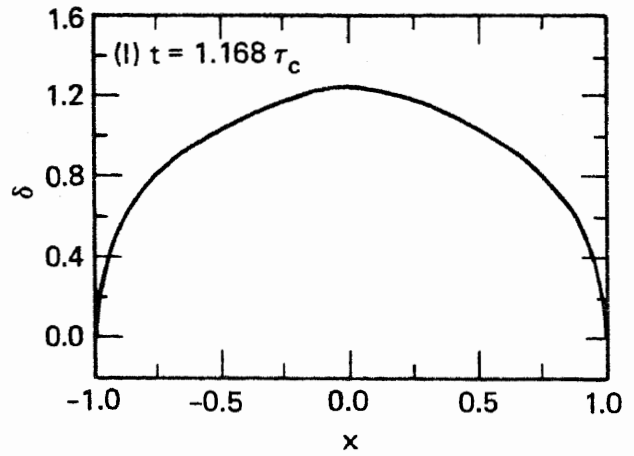
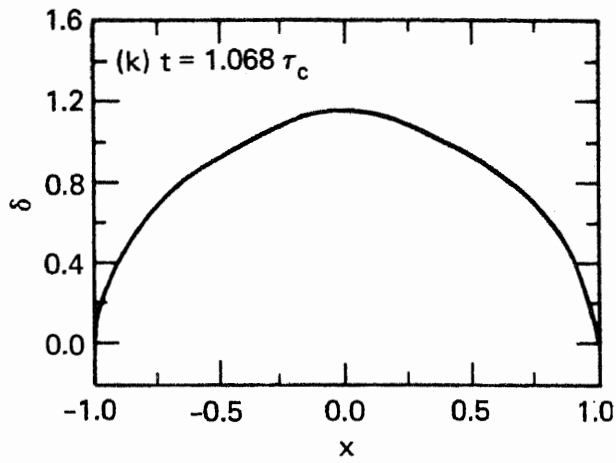


FIG. 11. Continued.

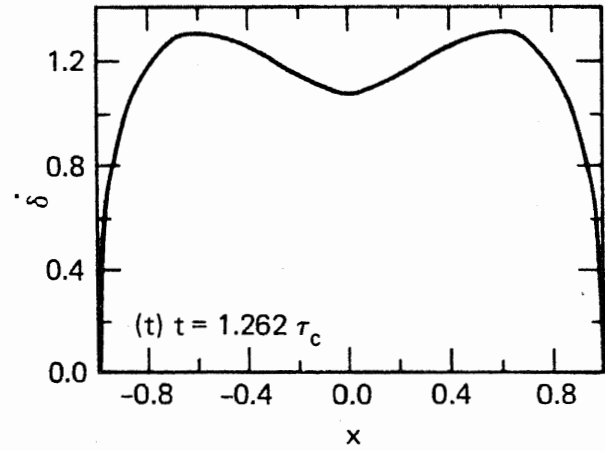
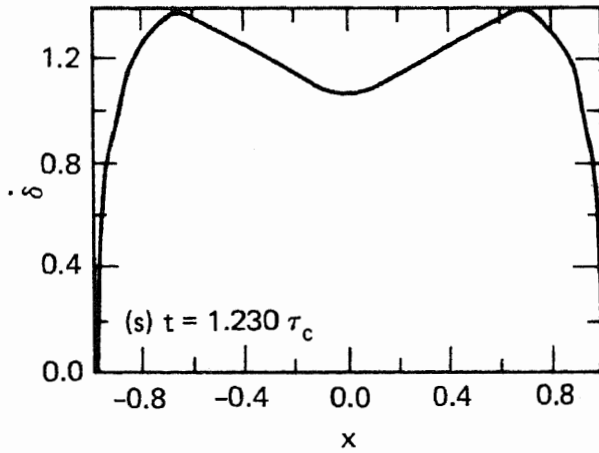
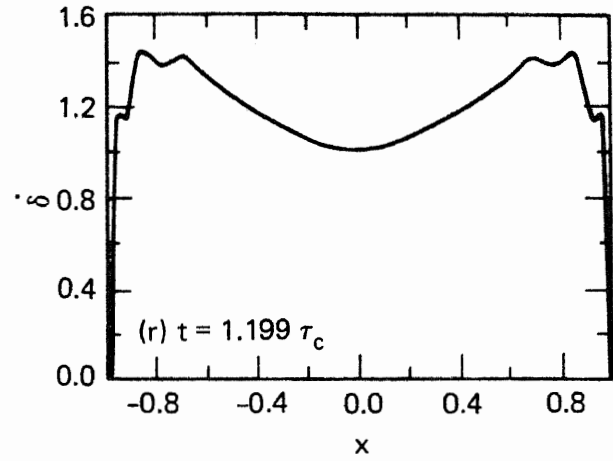
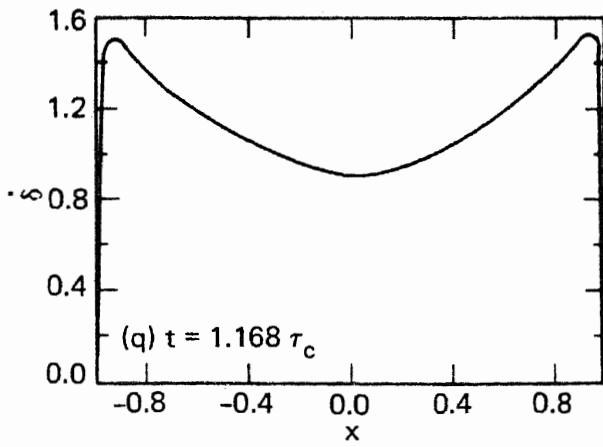


FIG. 11. Continued.

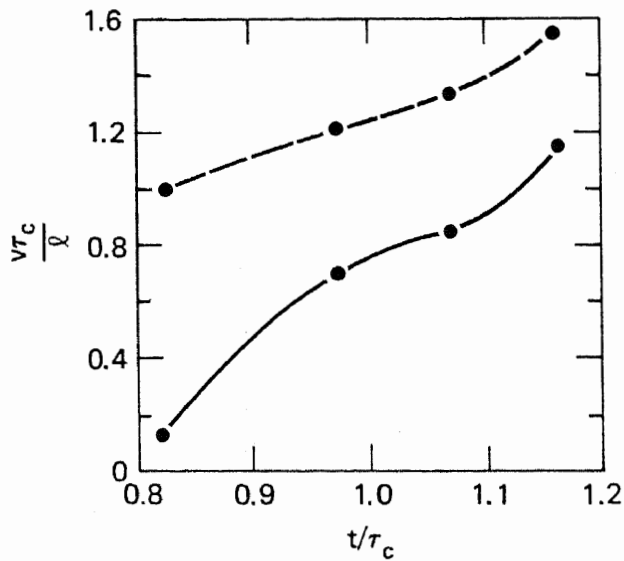


FIG. 12. Plot of fluid front velocity as a function of time (solid curve); (velocity of same fluid flowing between two parallel plates with spacing $\delta(x=0, t/\tau_0)$ and uniform pressure gradient ($P'/p_0 = 1.0$) is plotted as dashed curve).

this difference in velocities decreases somewhat, and seems to stabilize. We conclude that predictions of fluid-penetration times based on estimates of the crack opening and fluid pressure at the borehole may be quite conservative, but are of the right order to provide useful information. Thus, estimates based on τ_c , as given by Cleary,^{10,13} are useful guides to the process. We note, however, that such characteristic time estimates are easily made only in the case of a crack in a homogeneous medium with constant borehole pressure. It would be difficult, for instance, to include the effects of adjacent strata and inclusions. When our computer program is extended so that crack propagation in nonhomogeneous regions can be simulated, we will probably be able to develop correlations for τ_c based on numerical calculations.

EXPERIMENTAL

FRICITIONAL THRESHOLD EXPERIMENTS

We have continued to study the effects of friction on hydraulic fracture growth across an unbonded interface. The material used in these experiments was Indiana limestone. Earlier we reported¹² results on measurements of frictional characteristics of interfaces in dry and water-saturated Indiana limestone. The roughening of the interface surfaces in dry Indiana limestone by sandblasting did not significantly affect fracture penetration. However, the presence of water was found to alter the threshold normal stress for fracture growth across unbonded interfaces.

More recently we have investigated the use of lubricants on otherwise smooth, dry Indiana limestone interfaces. Two lubricants found to be effective in varying the frictional coefficient are HI TEMP C-100 Anti-Ball Lubricant* and 630-AA Lubriplate,[†] hereafter referred to as C-100 and 630-AA, respectively. Thin coatings of these lubricants were applied to the smooth surfaces of blocks of dry Indiana limestone, and friction experiments were performed using apparatus previously described.¹² The results of these experiments are presented in Fig. 13 along with previously reported results from experiments using dry and water-saturated Indiana limestone. Applied frictional stress necessary to initiate slip is plotted against normal interface stress. These two lubricants significantly decrease the friction on the interface. The C-100 lubricant produced more effective results. Data for 630-AA indicate more scatter and an apparent change of slope in the vicinity of 700-psi normal stress.

Hydraulic fracture experiments were then performed in which blocks of Indiana limestone were loaded in a 100-ton press as described earlier.¹² In these experiments a three-block sandwich arrangement was used. The hydraulic fracturing fluid was injected into the central block of the sandwich. One of the interior interfaces was coated with the lubricant; the other was kept dry as a control. Previous work had established a normal stress threshold of about 650 psi. Below this level a hydraulically driven crack would not cross a dry, unbonded interface in Indiana limestone. The present experiments established normal stress thresholds of about 1400 and 2200 psi for interfaces lubricated with 630-AA and C-100, respectively. Extrapolation of the friction data for the C-100 and 630-AA lubricants on limestone and for dry smooth limestone surfaces indicates that the interface must be able to support a shear frictional stress of 300–350 psi in order for a hydraulically driven crack to penetrate that interface. This critical shear threshold is about 40% of the tensile strength of the limestone as measured by Brazil tests.

FLUID FLOW EXPERIMENTS

Small-scale laboratory experiments are being performed to study the slow growth of penny-shaped cracks as a function of borehole pressure and applied closure stress. The experimental setup is shown schematically in Fig. 14. The effect of material toughness is removed by growing the "crack" in an interface

*Manufactured by FEL-PRO, Inc. Skokie, Illinois.

†Manufactured by Fiske Brothers Refining Co., Newark, New Jersey.

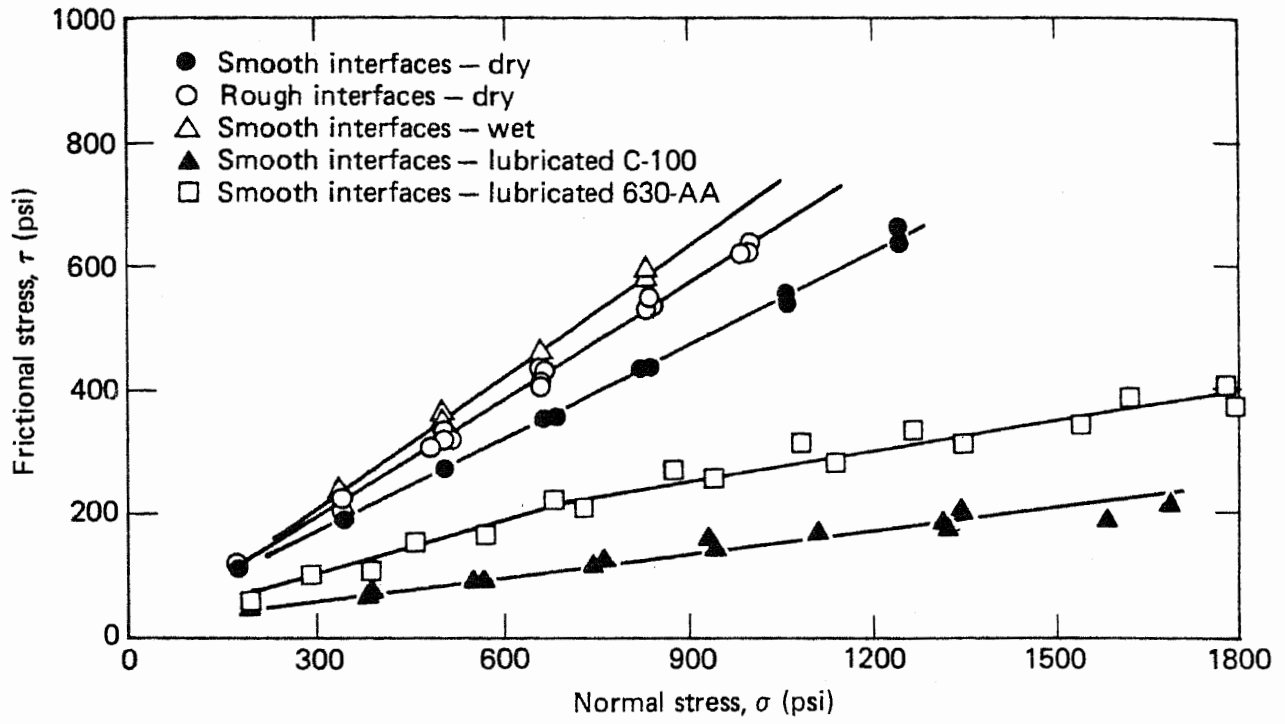


FIG. 13. Frictional plots of Indiana limestone.

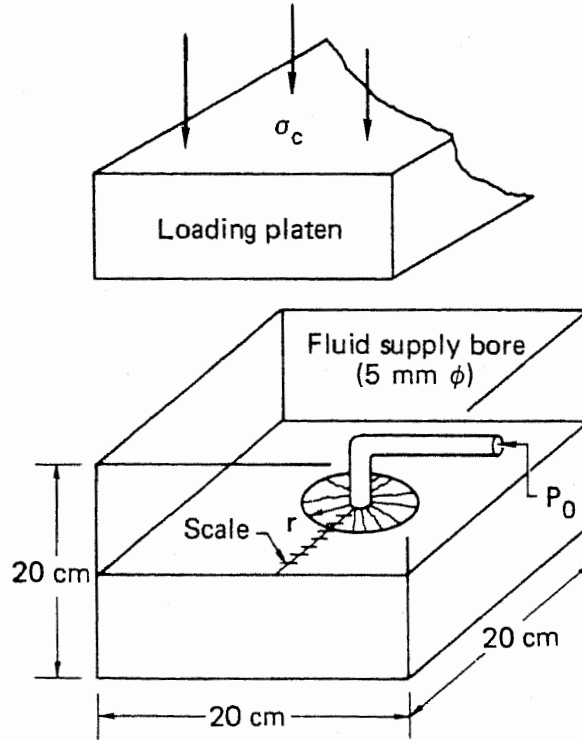


FIG. 14. Experimental setup for driving penny-shaped crack in PMMA.

between two blocks of polymethylmethacrylate (PMMA) which are pressed together by the applied closure stress, σ_c . A high viscosity ($\mu = 5 \times 10^2 \text{ Nsec/m}^2$) silicone fluid is used as a fracturing fluid to permit slow crack growth. A scale is scribed on one of the interface surfaces so that the rate of crack growth can be observed through the transparent PMMA.

The most general relationship, in nondimensional form, for the growth of the crack as a function of time is given by

$$\frac{tG}{\mu} = f\left(\frac{r}{r_0}, \frac{\sigma_c}{G}, \frac{p_0}{G}\right), \quad (20)$$

where r is the radius of the penny-shaped crack at time t , G is the elastic modulus, p_0 is the borehole pressure, σ_c is the closure stress, r_0 is the borehole radius, and μ is the viscosity of the fracturing fluid. The aim of the experiment is then to determine the functional form of f . Analysis has shown⁵ that the characteristic time of growth varies as $A(G/p_0 - \sigma_c)^3 \mu/G$. Thirty-six experiments were performed. An example of the data from two experiments is shown in Fig. 15. In these two experiments the effective pressure, $p_0 - \sigma_c$, was the same, (5×10^{-3}) G , but σ_c was different. These data show that with fixed effective pressure, crack growth was retarded by increasing σ_c . Preliminary analysis of all the data suggests the form

$$\frac{t\mu}{c} = \frac{\left(\frac{r}{20r_0} - 0.136\right)^{0.8}}{(1 - 0.136)^8} \left(\frac{G}{p_0 - c}\right)^3 c \left(\frac{\sigma_c}{G}\right). \quad (21)$$

More experiments and analyses are planned to further explore this relationship.

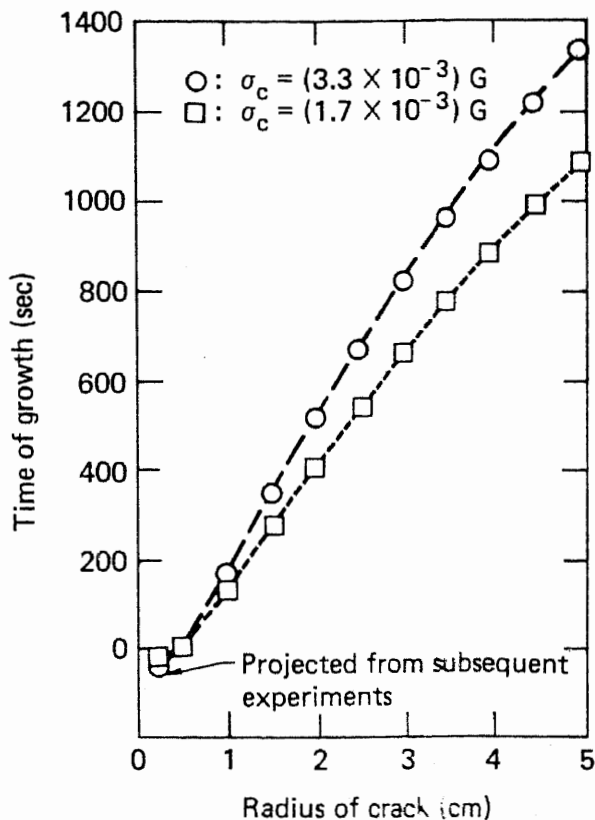


FIG. 15. Experimental results with constant effective pressure $p_0 - \sigma_c = (5 \times 10^{-3})G$, showing effects of varying confining pressure σ_c (borehole radius was 2.5 mm, $G = 10^9 \text{ N/m}^2$, $\mu = 6 \times 10^2 \text{ N-sec/m}^2$).

GEOLOGY AND GEOPHYSICS

DEVELOPMENT OF TIGHT WESTERN GAS SANDS

Introduction

This is a review of selected literature on the mechanics of the formation of joints in sedimentary rocks and on some analyses of jointing and the stress regime in the Rocky Mountain area. Similar reviews will cover tectonics and structure as they affect the accumulation of oil and gas in Rocky Mountain foreland basins that contain the important low-permeability "tight" gas sands. This work will be the basis for further analyses that may aid in exploration, development, and stimulation of the tight gas sands.⁵

An annotated bibliography and abstracts are appended to this review to serve as an introduction to the subject as it applies specifically to tight gas sands.

This work is based on the assumption that a fundamental knowledge of mechanical principles supported by laboratory data and field experience is necessary to analyze and to predict fracture location and formation. The rock environment and important physical parameters, past and present, must be measured or analyzed. To go beyond local empirical relationships requires rigorous analysis. As Turner and Weiss¹⁴ noted: "The theories of stress and strain are branches of the mechanics of continua. They deal mainly with the strictly continuous behavior of strictly homogeneous isotropic or anisotropic bodies under homogeneous or simple heterogeneous influences. Only in the most general way can they be applied to crystalline aggregates such as rocks; for these are strictly neither homogeneous nor spatially continuous, and seldom are isotropic."

Fracture Literature

Fractures or joints in rocks have been analyzed since the earliest geologic studies. Hodgson,¹⁵ who lists an extensive bibliography of earlier work, cites reports dating back to 1834. Considerable literature is noted in the late 19th century, with several titles relating to the origin of fractures. After 1920 the literature quickens and is enriched in the 1930's by the experimental work of D.T. Griggs and J. Handin and their students and co-workers. Price¹⁶ cites most of the earlier experimental and theoretical work on which our present ideas are based. Current investigation emphasizes the development of both theoretical and practical rock mechanics.

The importance of fractures in the accumulation and production of oil and gas has long been recognized. Levorson¹⁷ cites publications on the subject in the early days of the oil business—by E.B. Andrews in 1861, two years after the Drake well, and by T.S. Hunt in 1865 and I.C. White in 1883.

Recent oil and gas interest in fractures dates from about 1948 and the development of the fractured Spraberry Reservoir in west Texas.¹⁸ The Research Committee of the American Association of Petroleum Geologists sponsored a symposium on fractured reservoirs at its annual meeting in 1962.¹⁹ A selection of papers through 1973 was reprinted by the AAPG in 1977.²⁰ This reprint included important contributions sponsored by the research laboratories of Esso Production Research Company, Shell Development Company, Carter Oil Company, Gulf Oil Company, and the U.S. Geological Survey. The most recent report on tight gas sand area concerns fractured Cretaceous reservoirs in the San Juan Basin.²¹

We have been selective in that the literature reviewed, and particularly that abstracted and annotated herein, is pertinent to the conditions obtaining in the tight gas sands. Earlier reviews are noted, especially those with comprehensive bibliographies.^{16,22}

The following studies are the basis of this review and are listed in Appendix A with an annotated bibliography and abstracts:

1. Jointing and Fractures—General and Theoretical Mechanics of Hydraulic Fracturing—Hubbert and Willis²³
Fault and Joint Development in Brittle and Semi-Brittle Rock—Price¹⁶
Reservoirs in Fractured Rock—Stearns and Friedman²²
The Development of Stress Systems and Fracture Patterns in Undeformed Sediments—Price²⁴
Stress History and Rock Stress—Voight and St. Pierre²⁵
Significant Geologic Processes in Development of Fracture Porosity—Currie²⁶

2. Theoretical Studies of Jointing—Rocky Mountain Areas

Relation of Deformational Fractures in Sedimentary Rocks to Regional and Local Structure—Harris, Taylor, and Walper²⁷

Regional Study of Jointing in Comb Ridge: Navajo Mountain area, Arizona and Utah—Hodgson¹⁵

Quantitative Fracture Study: Sanish Pool, McKenzie County, North Dakota—Murray²⁸

Crustal Stress and Global Tectonics—Raleigh²⁹

Tight Gas Sands

“Tight gas sands” is a term used for the low-permeability reservoirs in the Rocky Mountain region. This catch-all term has been used for several quite distinct types of reservoirs, including the Upper Cretaceous shaly sandstones of the Northern Great Plains, the Wattenberg field in Colorado, and the Cretaceous in the San Juan Basin in New Mexico. We are here concerned with a widespread, very important subtype found in the Greater Green River, Uinta, and Piceance basins in Upper Cretaceous Mesaverde rocks and the Eocene Wasatch Formation. The structural geology and the tectonic histories of the basins are similar. Although the Wasatch is distinctly different from the underlying Mesaverde rocks, they share location and tectonic history in these areas. Although these gas-containing reservoirs contain large amounts of gas, they are difficult to develop because permeabilities commonly measure only a few microdarcies. The following are pertinent features listed in an earlier summary⁵:

- (1) The reservoirs are generally fine-grained, poorly sorted, and discontinuous.
- (2) Thick sedimentary sections are evidence of rapid sedimentation and burial.
- (3) Deformation is moderate in the areas of tight gas accumulation, with generally gentle folding and a small amount of associated faulting.
- (4) Heat flow is moderate and there has been little igneous activity within the basins of interest. This contrasts with the surrounding regions. The basins are generally aseismic.
- (5) Post-depositional history has included one or more cycles of uplift, reburial, and uplift.

These particular conditions and this history form a set of boundary conditions for the study of the mechanics of fracturing in the reservoirs of interest.

Stresses in Rock

Stresses underground are by convention considered compressive and can be referred to as three mutually perpendicular “principal” stress directions, one of which is taken as vertical, and two are horizontal. Except in the special case of pure hydrostatic stress, the principal stresses are unequal. On any surface within the rock, the stresses can be readily resolved into one *normal* (compressive) component perpendicular to the surface, and one *shear* component parallel to the surface.²³

The orientation of the stresses, according to Hubbert and Willis, will determine the type of shear deformation (faulting) that will occur. Reasons for this are (1) extension fractures tend to form in a plane normal to the least principal stress and (2) shear fractures tend to form parallel to the axis of intermediate stress and at acute angles to the greatest stress. Then, as shown in Fig. 16, three general results can occur:

- With the greatest stress vertical and the least and intermediate stresses horizontal, failure through faulting will be by steeply dipping shears, or “normal” faults.
- If the least stress is vertical and the other two are horizontal, with a compression or shortening in the direction of greatest stress, the result will be low-angle shear fractures, or “overthrust” faults.
- If both the greatest and least stresses are horizontal, the result will be vertical shears, called “transcurrent” or “strike-slip” faults.

These notions are simplified; natural systems, particularly small-scale structures or joints, are much more affected by local conditions. They do, however, provide a simple visual picture that aids our understanding of the more complex systems.

Hubbert and Willis point out that extension fractures, such as those made by injecting fluids under pressure, tend to form perpendicular to the direction of least principal effective stress. This simple notion is very important in consideration of natural and artificial joints.

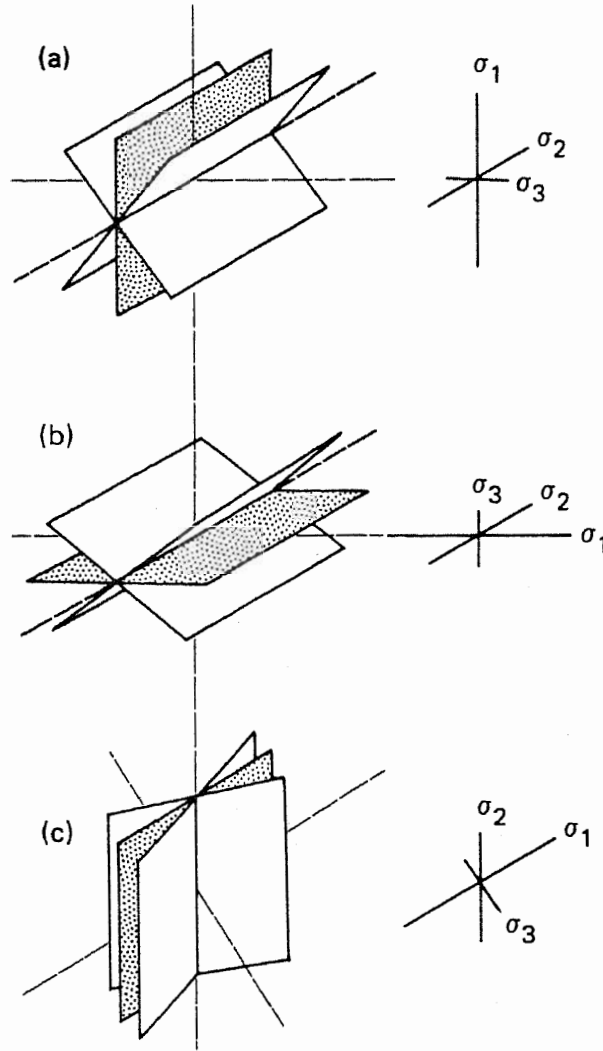


FIG. 16. Simple stress and fracture relationships: (a) Normal faults; (b) Overthrust faults; (c) Strike-slip faults (extension fractures are cross-hatched).

Secor³⁰ extended the work of Hubbert and others, emphasizing the importance of pore fluid pressure as a component of the stress system. The important value here is effective stress: the (algebraic) sum of the pore pressure and the applied stress. Secor has noted: "During a cycle of sedimentary accumulation and in the subsequent deformation a number of processes are operative which tend to increase the ratio of fluid pressure to overburden weight (and reduce the effective stress)—a Mohr stress circle will be repeatedly driven against the failure envelope." Either shear or extensional fracturing will occur. Currie²⁶ has noted: "Analysis of geologic conditions which favor natural extension fracturing in the subsurface illustrates that high pore pressure increases the depth to which extension fractures would be expected in basinal sedimentary deposits. This analysis suggests that regional overpressures could aid not only in creating fractures but also in maintaining them as open channels within a network of fracture permeability."

This pore pressure effect may be of great importance in the tight gas sand area. It provides a mechanism for jointing without major tectonic structures. The burial-loading-unloading history of the region is favorable and field data³¹ show that the low-permeability Mesaverde sandstones are moderately overpressured as in the deeper or lower parts of the Wamsutter Arch district of the Green River Basin. (See Fig. 17).

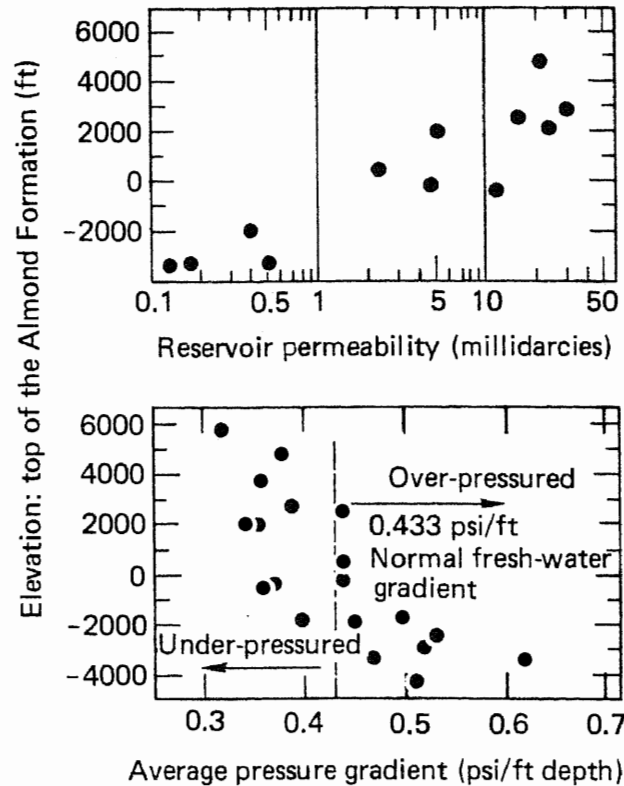


FIG. 17. Mesaverde Reservoir pressures and permeabilities, Wamsutter Arch, Wyoming (data from Wyoming Geological Association, 1979).

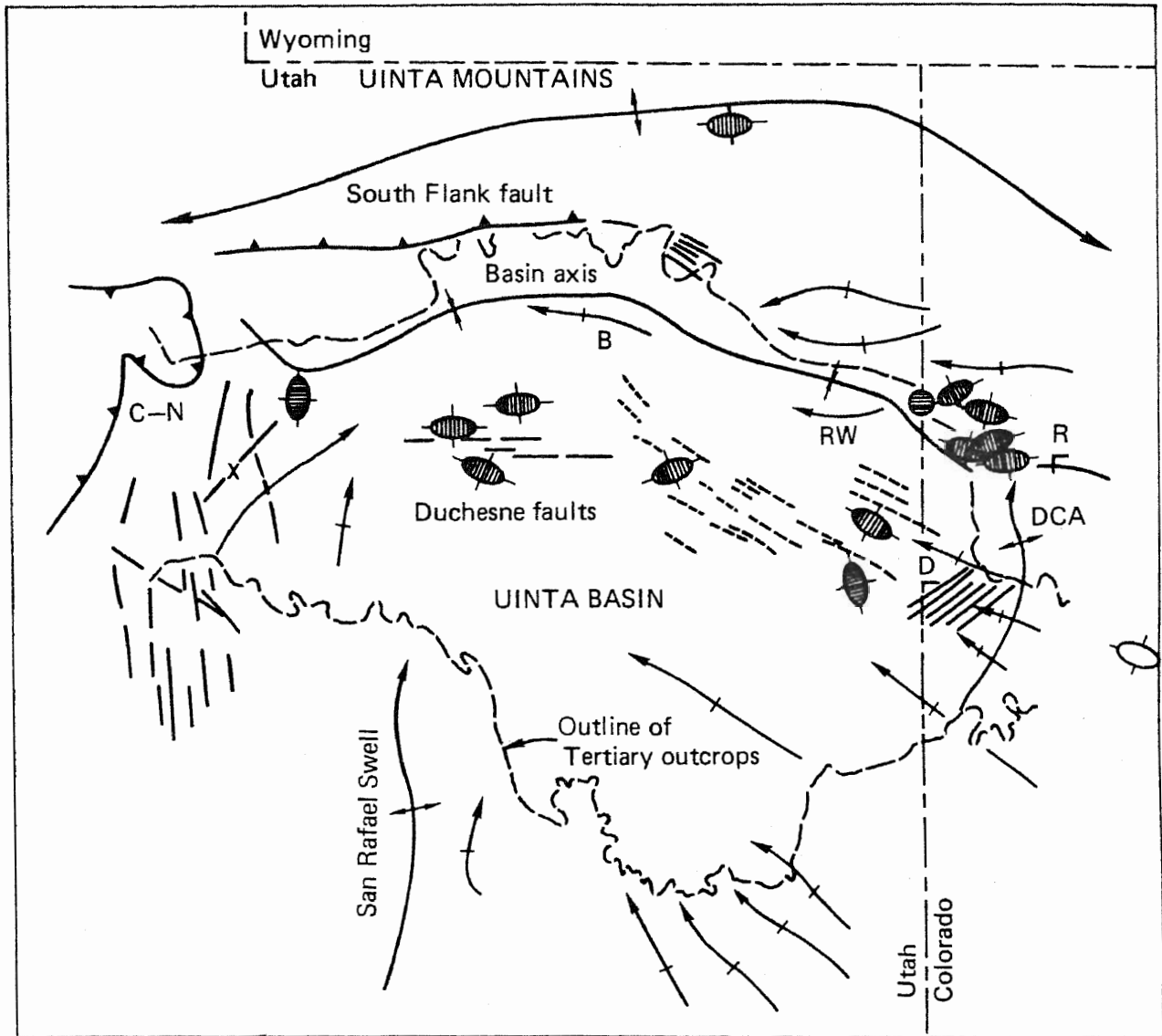
In summary, the principles of mechanics as applied to stresses and fractures within the earth can provide a rigorous theoretical framework for a discussion of fracture occurrences, orientations, and causes. Some of these, as has been pointed out, are of special interest to studies of the tight gas sand areas.

Regional and Local Stresses

Perhaps the only generalization that can be made about the areas covered by "regional" and "local" stresses is that large regional strains (structures) are a response to regional stress, and that the area covered by a more or less constant stress field can be related to the size of the strain effects being considered. Very small structures (e.g., joints) relate to "local" stresses. Field examples seem to indicate a complete spectrum. Recent history and the present stress patterns do not necessarily remove evidence of earlier responses to stress. Care must be used in attempting to determine present stress and probable strain (fracture) patterns from analysis of rock structures. This may be particularly true in tight gas sand areas such as the Green River and Uinta basins, where the present tectonically quiescent strain-relaxed environment is superposed on rocks and structures that are the result of a long and varied stress history.

Many statements on this subject may beg the question. The tectonic literature is replete with interpretations of stress from the study of geologic structures. Depending on the scale, these interpolations are often reused to demonstrate the congruence of certain other structures and the presumed stress field.

The difficulty is illustrated by comparing a regional compilation of field measurements of stress direction²⁹ with the geologic structures in the Uinta Basin area (Fig. 18). Simple interpretation of the basin shape and north boundary fault would suggest a north-south maximum stress direction, as would the trend of many of the folds. But the general east-west maximum stress direction correlated well with the regional uplifts (Douglas Creek Arch and San Rafael Swell). The extensional faulting near Duchesne matches the measured



Horizontal Stress Ellipse
 ● Maximum
 ○ Minimum
 — Normal and strike-slip faults
 ▽ Thrust faults - - - Gilsonite dikes
 + Anticlines
 20 miles

FIG. 18. Uinta Basin structure and *in situ* stress. DCA: Douglas Creek Arch; CN: Charleston-Nobo overthrust; B: Bluebell; D: Douglas Creek; R: Rangley; RW: Red Wash. After Raleigh²⁹ and Osmond.³⁵

stress directions nicely, whereas the gilsonite dikes (extension fractures?) lie at a considerable angle to the least horizontal stress direction. This may indicate that not only the geometry, but also the mode of formation is important, and that simple compressional-extensional theories of folding and faulting are not always useful.

Ode³² has shown that the complex dike pattern at Spanish Peaks, Colorado, could be interpreted as the result of the interaction of a local stress source (an intruding mass) with a regional compression. A local rigid boundary was also required. Much of the shallow deformation in the Rocky Mountain foreland area is dominated or modified by local systems that interact with regional patterns.³³ That is why simple analyses may not explain local details.

If the interpretation of minor structures such as joints in sedimentary rocks is correct, local stress in folded rocks may be dominated by sliding and bending forces rather than the larger stress field. Harris, Taylor, and Walper²⁷ in Wyoming, Murray²⁸ in the Williston Basin, and Gorham et al.²¹ in the San Juan Basin have shown that fracture orientation and intensity are related to intensity of folding or bed curvature. Stearns and Friedman²² have in addition shown that a second set of fractures may be formed during later phases of folding. This presumably is the result of reorientation of the operative local stresses.

Hubbert and Willis²³ demonstrated that hydraulic fractures should form approximately perpendicular to the least principal stress. They concluded that: "In geologically simple and tectonically relaxed areas, not only should the fractures in a single field be vertical but they also should have roughly the same direction of strike." Used with caution, this may be a useful working hypothesis. The tight gas sands are generally in simple, tectonically relaxed areas. The confidence we can have in stress-strain interpretations depends on the adequacy of the data describing the underground environment as compared to the complexity and the size of the field under investigation.

Factors Controlling Fractures

Stearns and Friedman²² listed three primary factors relating to fracture control:

- The physical environment including effective confining pressure, temperature, and strain rate
- The magnitudes and orientation of the three principal stresses
- The nature of the rock, including degree of induration and the thickness of the rock units

Stearns and Friedman concluded: "Though fracturing is a complicated process, laboratory and field studies provide as good a basis for estimating fracture development and trends as is available for many other geologic phenomena ...".

Price¹⁶ emphasized the importance of the changes in stress regime due to burial, uplift, and unloading. He later demonstrated that joints can be developed during downwarp and uplift without folding, as the flexures in downwarp and uplift are in themselves sufficient to cause tensile failure.²⁴ Retained pore pressure in less permeable rocks is important because it causes over-pressure upon uplift. These factors are also listed by Voight and St. Pierre²⁵ and Currie.²⁶

Price¹⁶ listed the effects of several variables:

Frequency. Joint frequency is many times fault frequency; a joint relieves stress only in its immediate vicinity.

Lithology. Joint frequency is greater in weaker rocks, e.g., coal vs sandstone. This appears related to strain energy stored in a body of elastic rock, inversely proportional to Young's modulus.

Bed Thickness. Frequency is inversely proportional to bed thickness, probably due to frictional forces between beds.

Tectonic Deformation. Normalized for lithology and thickness, frequency is directly related to bed curvature or rate of change of dip. Price cites Harris, Taylor, and Walper²⁷ and Murray.²⁸

Fracture Orientation

Orientation and length of fractures, whether natural or induced, are most important in determining their effect on well and reservoir performance. Determining fracture orientation is thus one of the two or three most important objectives of studies such as this. Following is a brief review of the evidence for the orientation of natural fractures vis-a-vis folding, together with some theoretical conjecture of their relation to the causative stresses. We consider fractures with little or no displacement parallel to the fracture surface ("joints" by definition), and only those resulting from brittle or semi-brittle failure. The last criterion excludes forms of foliation due to rock flowage, such as slaty or "axial plane" cleavage. Although the theoretical and laboratory

measured fractures are related to stress as shown in Fig. 16. many local details may change or rotate the stress field.

Stearns and Friedman²² discuss the general relationships shown in Fig. 19, where the jointing-to-folding relationship is illustrated. Those joints related to faulting would be caused by the same stress system and are of similar or complementary orientation to the fault. They are not very relevant to the tight gas sand problem in the simple structures within the Rocky Mountain basins.

Two systems of joints are recognized:

(1) One set (one extension fracture and two shears) is oriented with the extensional fracture parallel to the dip direction, or on the flanks of a fold, perpendicular to the fold axis. Joints are formed during early or moderate folding.

(2) A similar set, oriented perpendicular to the first and generally parallel to fold axes, is formed during later or more intense deformation.

The fractures are perpendicular to bedding planes. With consideration of rock quality and bed thickness, these concepts could be guidelines for new exploration. Type (1) orientation might be found on the gentler structures, such as Wyoming's Wamsutter Arch, that are often associated with the tight gas sands. Harris, Taylor, and Walper²⁷ show field examples of patterns from Wyoming that appear to be type (2) in strongly folded rocks.

Hodgson¹⁵ found two sets of joints in gently folded rocks in the Colorado Plateau, and called on earth tides to provide the required stress. Price²⁴ demonstrated that fractures could be formed by flexures of downwarp and uplift field examples show this. Note the orientation shown in Fig. 20. Note also the correlation with basin axis or direction of maximum flexure which is similar to our type (1) in folded terranes.

These relationships might be used, with adequate site-specific data, to extrapolate fracture patterns laterally or into the subsurface, or to estimate directions of principal stress.

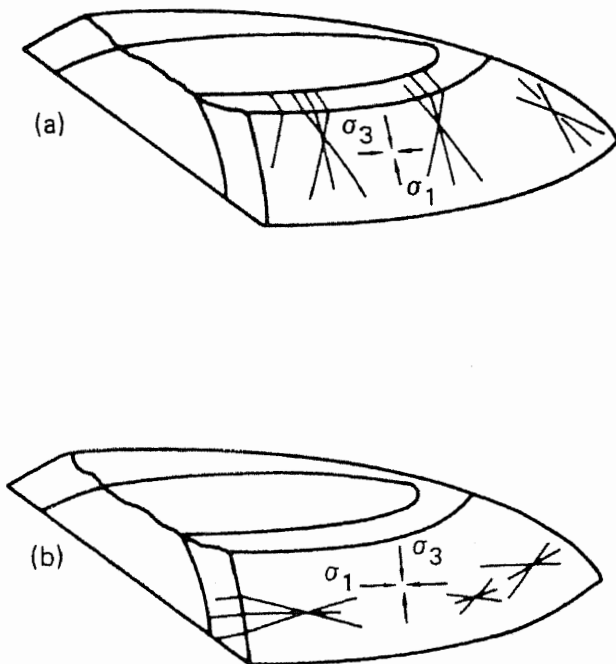


FIG. 19. Fractures commonly dissociated with (a) early and (b) late folds (after Stearns and Friedman²²).

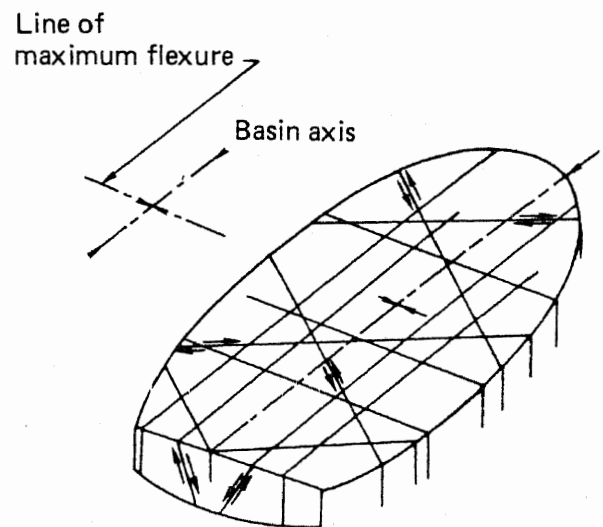


FIG. 20. Fracture patterns that may form without folding, showing orientation of fractures that may form during one cycle of downwarp and uplift (after Price²⁴).

Summary

Data on natural rock fractures and measurement or estimates of stress show promise as an aid in predicting the orientation and continuity of both natural and artificial fractures in natural gas reservoirs. Overbey and Rough,³⁴ for instance, have shown that one set of surface joints in the Bradford field in Pennsylvania nearly parallels the direction of artificial hydraulic fractures in the reservoir.

The "tight gas sands" in the Rocky Mountains are thin, discontinuous, and have low permeability. They are found in gently folded rocks and often have abnormally high pore pressure.

In a relaxed tectonic setting, one principal stress is most often nearly vertical, and the other two are horizontal. Natural fractures usually approximate the same orientation to stresses as those produced experimentally. Increased pore pressure extends the depth to which extensional fractures can occur, and these tend to form perpendicular to the direction of the least principal stress.

Local stresses that control small features such as joints may be different from, although compatible with, regional stress. In folded rocks, sliding and bending forces appear to be most important in forming the smaller structures such as joints. Fractures can be formed by flexing during downwarp and uplift; more intense folding or faulting is not necessary.

Fractures are controlled by the physical environment, the stresses, and the nature of the rock. Changes in stress due to burial and uplift are also important. Jointing frequency is greater in weak and thinly bedded rocks and is directly related to intensity of folding.

Two sets of both shear and extensional fractures may develop: one oriented parallel, the other, normal to axes of folding or downwarp. These relations may be used to extrapolate fracture patterns laterally or into the subsurface.

ROCK MECHANICS MEASUREMENTS

Current methods for predicting intensity, geometry, and extent of fracturing resulting from high-explosive or hydraulic stimulation of an initially impermeable natural gas-bearing rock require certain equation-of-state (EOS) measurements as input data to the calculation codes. We have continued to generate the required EOS data for Mesaverde sandstone (reservoir rock) and shale (source rock) core sections from the Twin Arrow well, No. C&K 4-14 in Rio Blanco, Colorado, and the Federal No. 24-19 well in Sublette County, Wyoming. The depth of sample origin ranged from 349.9 to 354.5 m for the Colorado well and from 1579.9 to 1582.8 m for the Wyoming well.

The core sample contains alternating sections of sandstone, shale, and a mixture of the two. The sandstone sections are quite homogeneous. The bedding planes between sandstone and shale are horizontal (perpendicular to the axis of the core sample). However, within the sections of pure sandstone or shale, the bedding is not obvious. For the Colorado rocks, the shale sections show different colors at different depths. At 349.9 m the shale is black-gray; at 351 m it becomes gray; at 354 m it contains bands of yellow-gray; at 358 m the shale is pure gray. For the Wyoming rocks, the colors of the sandstone and shale are light gray and dark gray, respectively. The sandstone is very fine grained.

To date we have completed the pressure-volume measurement for the Mesaverde shale from Rio Blanco County, Colorado. The specimens were right cylinders of about 1.27-cm diameter and 2.54-cm length, cored either parallel or perpendicular to bedding. Volumetric strain as a function of confining pressure, up to a pressure of 1.2 GPa, was determined by strain measurements of longitudinal and radial strain gages. Typical data of pressure-volume measurements are shown in Figs. 21 and 22. These are the pressure-volume data of the first pressure cycle. Figure 21 shows the data of one specimen cored parallel to bedding; Fig. 22 shows the data of another specimen cored perpendicular to bedding. These data were fitted to polynomial functions by the least square methods. The results of the fits for these two specimens during the increasing pressure cycle are:

SH-106 (Fig. 21), $-\Delta V/V_0 = 0.1773 + 0.5633 P - 0.02213 P^2$, with one standard deviation of 0.0113%,
SH-42 (Fig. 22), $-\Delta V/V_0 = 0.0597 + 0.4175 P - 0.0099 P^2$, with one standard deviation of 0.00253%,
where $\Delta V/V_0$ is in percent and P is in kilobars.

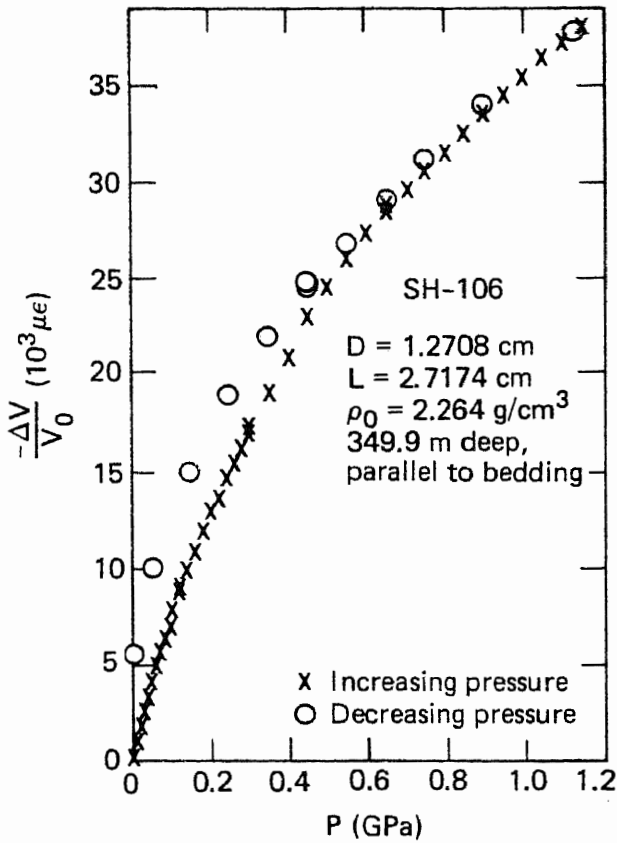


FIG. 21. Pressure-volume relationships for mesaverde shale cored parallel to bedding. SH-106: D = 1.2708 cm; L = 2.7174 cm; $\rho_0 = 2.264 \text{ g/cm}^3$; depth = 349.9 m.

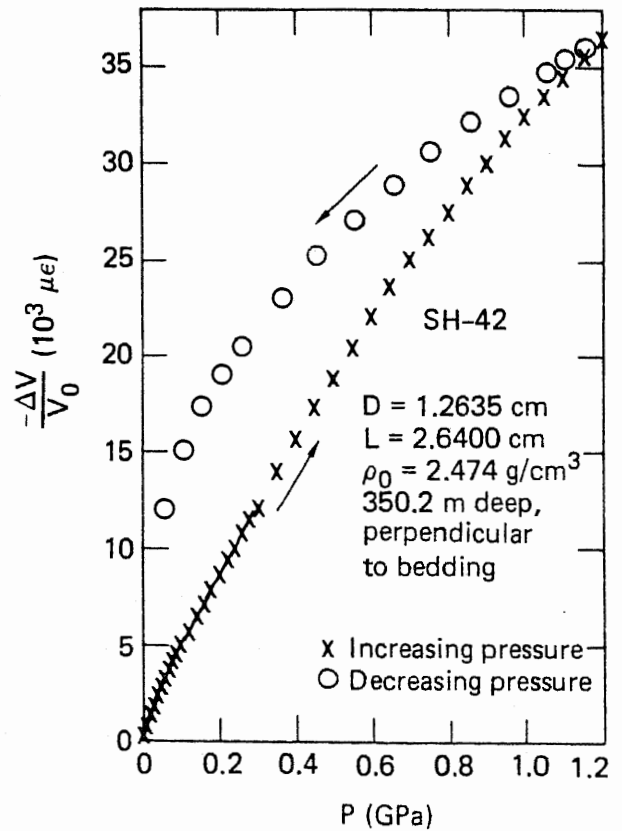


FIG. 22. Pressure-volume relationships for mesaverde shale cored perpendicular to bedding. SH-42: D = 1.2635 cm; L = 2.6400 cm; $\rho_0 = 2.474 \text{ g/cm}^3$; depth = 350.2 m.

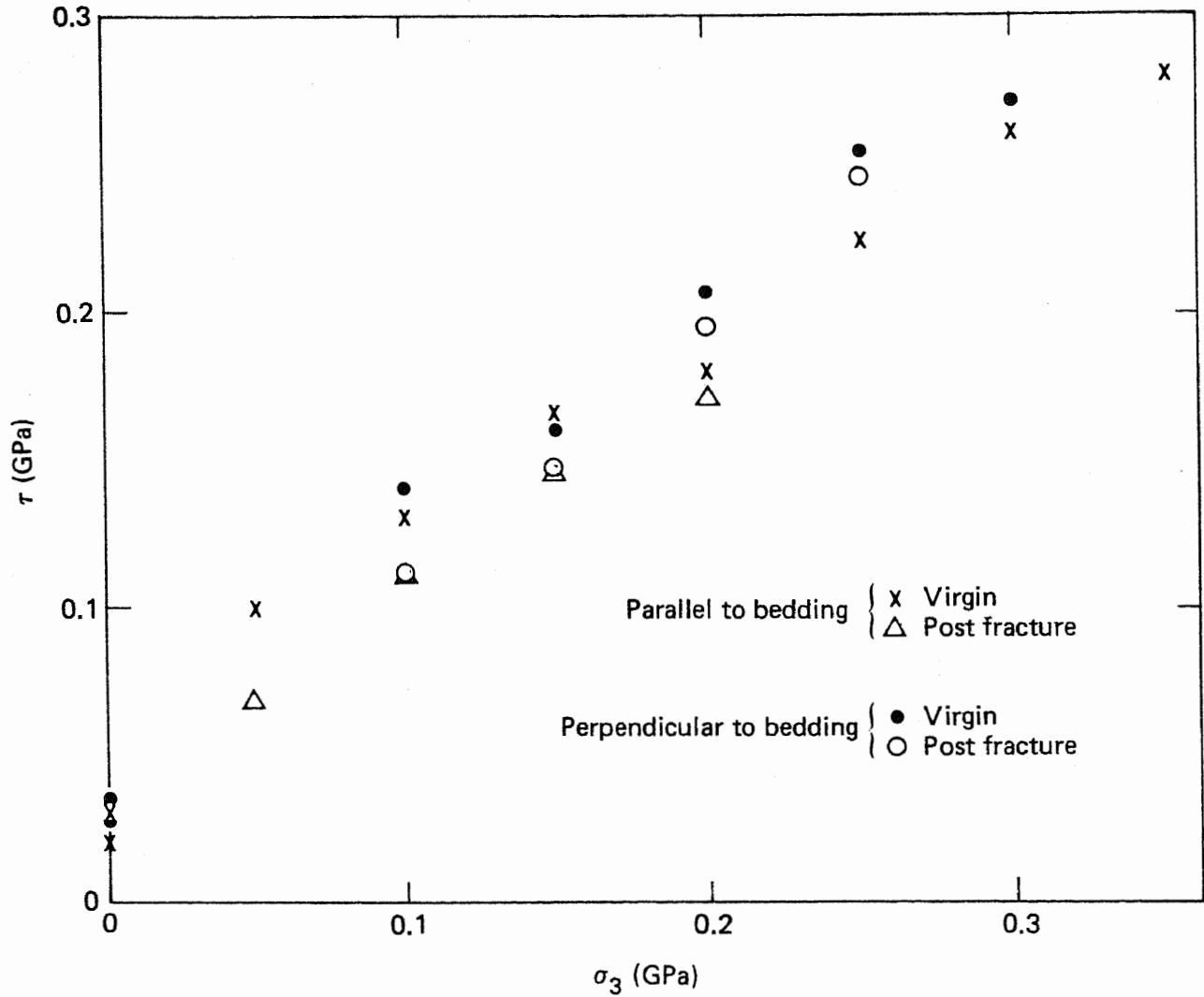


FIG. 23. Failure envelopes of mesaverde sandstone, Sublette County, Wyoming (depth = 1582.2 m).

We have also completed the failure envelope study for the Mesaverde sandstone from Sublette County, Wyoming. The results of this study are shown in Fig. 23. The specimens loaded perpendicular to bedding have slightly greater compressive strength than those loaded parallel to bedding. However, the difference is not significant, especially at low confining pressure.

REFERENCES

1. C. R. McKee, M. E. Hanson, and R. W. Terhune, *Permeability from Single and Multiple Detonations of Explosive Charges*, Lawrence Livermore Laboratory, Livermore, Calif., UCRL-78207, Rev. 1 (1976).
2. M. E. Hanson, G. D. Anderson, R. J. Shaffer, D. N. Montan, L. D. Thorson, W. Lin, B. C. Haimson, and M. P. Cleary, *LLL Gas Stimulation Program Quarterly Progress Report October through December 1978*, Lawrence Livermore Laboratory, Livermore, Calif., UCRL-50036-78-4 (1979).
3. M. E. Hanson, G. D. Anderson, R. J. Shaffer, D. O. Emerson, R. P. Swift, K. O'Banion, M. P. Cleary, B. Haimson, C. F. Knutson, and C. R. Boardman, *LLL Gas Stimulation Program Quarterly Progress Report July through September 1978*, Lawrence Livermore Laboratory, Livermore, Calif., UCRL-50036-78-3 (1978).
4. M. E. Hanson, G. D. Anderson, R. J. Shaffer, J. R. Hearst, B. Haimson, and M. P. Cleary, *LLL Gas Stimulation Program Quarterly Progress Report April through June 1978*, Lawrence Livermore Laboratory, Livermore, Calif., UCRL-50036-78-2 (1978).
5. M. E. Hanson, G. D. Anderson, R. J. Shaffer, D. F. Towse, J. R. Hearst, W. Lin, and M. P. Cleary, *LLL Gas Stimulation Program Quarterly Progress Report July through September 1979*, Lawrence Livermore Laboratory, Livermore, Calif., UCRL-50036-79-3 (1979).
6. J. E. Welch, F. H. Harlon, J. P. Shannon, and B. J. Daly, *The Mack Method*, Los Alamos Scientific Laboratory, Los Alamos, New Mexico, LA-3425 (1965).
7. J. A. Viecelli, "A Computing Method for Incompressible Flows Bounded by Moving Walls," *J. Comp. Phys.* **8** (1971).
8. I. N. Sneddon and M. Lowengrub, *Crack Problems in the Classical Theory of Elasticity* (John Wiley and Sons, Inc., New York, 1969).
9. A. A. Denesny, *Opening of a Pressurized Fracture in an Elastic Medium*, Petroleum Society of CIM, Paper No. 7616 (1971).
10. M. P. Cleary, "Rate and Structure Sensitivity in Hydraulic Fracturing of Fluid-Saturated Porous Formations," to appear in the *Proc. 20th U.S. Symp. on Rock Mechanics, University of Texas at Austin, June 1979*.
11. M. E. Hanson, G. D. Anderson, R. J. Shaffer, D. F. Towse, A. G. Duba, N. R. Burkhard, W. Lin, M. P. Cleary, and B. C. Haimson, *LLL Gas Stimulation Program Quarterly Progress Report January through March 1979*, Lawrence Livermore Laboratory, Livermore, Calif., UCRL-50036-79-1 (1979).
12. M. E. Hanson, G. D. Anderson, R. J. Shaffer, W. Lin, D. F. Towse, M. P. Cleary, and B. C. Haimson, *LLL Gas Stimulation Program Quarterly Progress Report April through June 1979*, Lawrence Livermore Laboratory, Livermore, Calif., UCRL-50036-79-2 (1979).
13. M. P. Cleary, *Primary Factors Governing Hydraulic Fractures in Heterogeneous Stratified Porous Formations*, ASME Paper No. 78-PET-47 (1978).
14. F. J. Turner and L. E. Weiss, *Structural Analysis of Metamorphic Tectonites* (McGraw-Hill Publishing Company, New York, 1963).
15. R. A. Hodgson, "Regional Study of Jointing in Comb Ridge—Navajo Mountain Area, Arizona and Utah," *Am. Assoc. Pet. Geol. Bull.* **45**, 1-38 (1961).
16. N. J. Price, *Fault and Joint Development in Brittle and Semi-Brittle Rock* (Pergamon Press, London, 1966).
17. A. I. Levorson, "Discussion of Fractured Reservoir Subjects," *Am. Assoc. Pet. Geol. Bull.* **37**, 314-330 (1953).
18. W. M. Wilkinson, "Fracturing in Spraberry Reservoir, West Texas," *Am. Assoc. Pet. Geol. Bull.* **37**, 250-265 (1953).
19. E. A. Koester and H. L. Driver, "Symposium on Fractured Reservoirs," *Am. Assoc. Pet. Geol. Bull.* **37**, 201-330 (1953).
20. J. R. Kostura and J. H. Ravenscroft, *Fracture-Controlled Production*, AAPG Reprint Series No. 21 (AAPG, Tulsa, 1977).

21. F. D. Gorham, Jr., L. A. Woodward, J. F. Callender, and A. R. Green, "Fractures in Cretaceous Rocks from Selected Areas of San Juan Basin, New Mexico—Exploration Implications," *Am. Assoc. Pet. Geol. Bull.* **63**, 598-607 (1979).
22. D. W. Stearns and M. Friedman, "Reservoirs in Fractured Rock," in *Stratigraphic Oil and Gas Fields*, AAPG Memoir 16 (AAPG, Tulsa, 1972), pp. 82-106.
23. M. K. Hubbert and D. G. Willis, "Mechanics of Hydraulic Fracturing," *J. Pet. Technol.* **210**, 153-163 (1957).
24. N. J. Price, "The Development of Stress Systems and Fracture Patterns in Underformed Sediments," *Proc. 3rd Congr. Int. Soc. Rock Mechanics* (National Academy of Sciences, Washington, D.C., 1974), Vol. 1, pp. 487-496.
25. B. Voight and B. H. P. St. Pierre, "Stress History and Rock Stress," *Proc. 3rd Congr. Int. Soc. Rock Mechanics* (National Academy of Sciences, Washington, D.C., 1974), Vol. 2, pp. 580-583.
26. J. B. Currie, "Significant Geologic Processes in Development of Fracture Porosity," *Am. Assoc. Pet. Geol. Bull.* **61**, 1086-1089 (1977).
27. J. F. Harris, G. L. Taylor, and J. L. Walper, "Relation of Deformation Features in Sedimentary Rocks to Regional and Local Structure," *Am. Assoc. Pet. Geol. Bull.* **44**, 1853-1873 (1960).
28. G. H. Murray, Jr., "Quantitative Fracture Study—Sanish Pool, McKenzie County, North Dakota," *Am. Assoc. Pet. Geol. Bull.* **52**, 57-65 (1968).
29. C. B. Raleigh, "Crustal Stress and Global Tectonics," *Proc. 3rd Congr. Int. Soc. Rock Mechanics* (National Academy of Sciences, Washington, D.C., 1974), Vol. 1, p. 597.
30. J. T. Secor, Jr., "Role of Fluid Pressure in Jointing," *Am. J. Sci.* **263**, 633-646 (1965).
31. Wyoming Geological Association, *Wyoming Oil and Gas Symposium Greater Green River Basin* (W.G.A., Casper, Wyoming, 1979), 2 vols.
32. H. Ode, "Mechanical Analysis of the Dike Pattern of the Spanish Peaks Area, Colorado," *Geol. Soc. Am. Bull.* **38**, 567-576 (1957).
33. J. D. Lowell, "Plate Tectonics and Foreland Basement Deformation," *Geology* **2**, 275-278 (1974).
34. W. K. Overbey, Jr., and R. L. Rough, "Surface-Joint Patterns Predict Well-Bore Fracture Orientation," *Oil Gas J.* **66**(9), 84-86 (1963).
35. J. C. Osmond, "Tectonic History of the Uinta Basin, Utah," in *Guidebook to the Geology and Mineral Resources of the Uinta Basin* (Intermountain Association of Petroleum Geologists, Salt Lake City, 1964), pp. 47-58.

APPENDIX A.

ANNOTATED BIBLIOGRAPHY WITH ABSTRACTS.

Currie, J.B., "Significant Geologic Processes in Development of Fracture Porosity," *Am. Assoc. Pet. Geol. Bull.* **61**, 1086-1089 (1977).

Abstract

Folding and faulting should be regarded as only two of the several geologic processes that originate fracture porosity. Geologic evidence advanced by Currie and Nwachukwu supports the view that regional uplift and erosional unloading of strata also contribute to development of open fractures in the subsurface. In addition, studies by Magara demonstrated that regional paleo-overpressure could be a significant factor in the origin of fracture porosity. These regional processes may influence a fractured reservoir significantly, for example, by helping to maintain open fractures and, thereby, to enhance fracture permeability.

Discussion

This "Geologic Note" gives a brief review and a good bibliography of recent work.

It emphasizes that jointing can develop without folding or faulting, that overpressure can facilitate fracturing, and that relaxation of pressure may lead to reduction in fracture permeability.

Burial, regional uplift, and erosional unloading are characteristic of the post-Cretaceous history in the western tight gas sand regions.

Currie cites examples of recent work in the Cretaceous section in Alberta.

Harris, J.F., G.L. Taylor, and J.L. Walper, "Relation of deformation features in sedimentary rocks to regional and local structure," *Am. Assoc. Pet. Geol. Bull.* **44**, 1853-1873 (1960).

Abstract

Surface studies of fractures, on both local and regional compressional structure, show a definite relation between the trend of the fractures, their density, and the structure on which they occur.

The susceptibility of any stratum to fracturing is dominantly controlled by the thickness and lithologic character of the stratum. These factors are evaluated and used to convert fracture data taken on beds of various lithologic character and thickness to a datum bed. Fracture-pattern and iso-fracture maps are then constructed from these data.

These methods were applied in the field to two areas in Wyoming: the Goose Egg dome of local extent and the sheep Mountain area of regional extent. These areas show that the trend and concentration of fractures are controlled by the compressional structure configuration.

Plots of the strikes and densities of joints reveal two sets of fractures making in general a small angle with fold axes, and with a density related to degree of folding. Data have been normalized for bed thickness and lithologic type.

Discussion

Although the writers describe the structures as compressional and use only major through-going fracture sets that they designate "of compressional origin," the relation to the compression that formed the folds is not clear. In fact, the acute angle between the (shear?) fractures indicates that the maximum compressive stress is *parallel* to the fold axes. This is not to detract from the usefulness of the relationships, but only to indicate more analyses could be made. Dip of fractures is not shown, so we cannot know exact attitude. The fractures shown appear to be one of the sets shown by Stearns and Friedman²² that they relate to later, more intense folding.

This is a field example of fracture relationships with folding in the Rocky Mountain foreland area of interest. The origin, the relationship of regional stresses, and the extent of basement involvement in these folds are still controversial, as a review of the literature on Rocky Mountain structures and tectonics will show. Consequently, a convincing analysis of the mechanical origin of the fractures will be difficult.

Hodgson, R.A., "Regional study of jointing in Comb Ridge—Navajo Mountain Area, Arizona and Utah," *Am. Assoc. Pet. Geol. Bull.* **45**, 1-38 (1961) (reprinted in *Fracture-Controlled Production*, AAPG Reprint Series No. 21, AAPG, Tulsa, 1977).

Abstract

The spatial relations of joints and, in particular, structural details of individual joints, offer clues of their origin. Important features of joints have been largely neglected in previous joint studies; the present study is an attempt to determine more closely the true nature of joints in sedimentary rocks and to suggest a mode of origin more in line with field observations than is present theory.

The study area comprises about 2,000 square miles of the Colorado Plateau in northeastern Arizona and southeastern Utah where sedimentary rocks ranging from Pennsylvanian to late Cretaceous in age are exposed.

A simple, nongenetic joint classification is presented based on the spatial relations of joints and the plumose structures on joint faces. Joints are grouped as systematic or non-systematic with cross-joints defined as an important variety of non-systematic joints.

Plumose structures on joint faces indicate that joints are initiated at some structural inhomogeneity within the rock and propagated outward, thus precluding movement in the direction of the joint faces at the time of formation. Spatial relations of systematic joints point to formation at or near the earth's surface in a remarkably homogeneous stress field.

The regional joint pattern is composed of a complex series of overlapping joint trends. The pattern as a whole extends through the entire exposed rock sequence. Intersecting joint trends have no visible effect on each other and may terminate independently in any direction. Each joint trend of the regional pattern crosses several folds of considerable magnitude, but does not swing to keep a set angular relation to a fold axis as the axis changes direction.

Hypotheses stating that joints are related genetically to folding are rejected for the mapped area. The shear, tension, or torsion theories of jointing require that only one or two sets of joints be considered as the result of a particular stress condition. Where more sets are present, different stress conditions must be postulated for each set or pair of sets believed to be related genetically. The joint pattern in the mapped area cannot be interpreted in such terms without making these assumptions. Alternatively, in accord with theoretical and experimental evidence, semidiurnal earth tides are considered as a force capable of producing joints in rocks through a fatigue mechanism. Field observations suggest that joints form early in the history of a sediment and are produced successively in each new layer of rock as soon as it is capable of fracture. The joint pattern in preexisting rocks may be reflected upward into new, nonjointed rock and so control the joint directions.

Critical data from areas with different geologic histories are needed before a quantitative evaluation of this hypothesis can be made. The question of the ultimate origin of the regional joint pattern and its genetic relation, if any, to other structure at depth can not be answered on data now available.

Discussion

This is a valuable set of regional data, but a more satisfactory explanation than fatigue cracking because of earth tides should be possible using the results of later work; e.g., Price^{16,24}; Stearns and Friedman.²²

The nongenetic classification describes joints only by their geometry, consistency, spacing, and relation to each other. Hodgson noted here the general dip of joints at about 90 deg to bedding planes.

A cursory examination of his map seems to show two sets of joints in an area—each, perhaps, with a different origin. One may be due to downwarp uplift²⁴; another may be related to fold geometry.²²

Fold axes are generally parallel to one of two general fracture directions, N-S and NW-SE. Another set, E-W and NE-SW, could be interpreted as a shear set with a maximum principal stress perpendicular to most fold axes. Where fold structure is simpler, in the northeast part of the map area, so is jointing. One set is apparently not developed.

Hubbert, M.K., and D.G. Willis, "Mechanics of Hydraulic Fracturing," *J. of Pet. Technolo.* **210**, 153-163 (1957) (reprinted in *Underground Waste Management and Environmental Implications*, AAPG Memoir 18, AAPG, Tulsa, 1972, and *Fracture-Controlled Production*, AAPG Reprint Series No. 21, AAPG, Tulsa, 1977).

Abstract

A theoretical examination of the fracturing of rocks by means of pressure applied in boreholes leads to the conclusion that, regardless of whether the fracturing fluid is of the penetrating or nonpenetrating type, the fractures produced should be approximately perpendicular to the axis of least stress. The general state of stress underground is that in which the three principal stresses are unequal. For tectonically relaxed areas characterized by normal faulting, the least stress should be horizontal; the fractures produced should be vertical, and the injection pressure should be less than that of the overburden. In areas of active tectonic compression, the least stress should be vertical and equal to the pressure of the overburden; the fractures should be horizontal, and injection pressure should be equal to, or greater than, the pressure of the overburden.

Horizontal fractures cannot be produced by hydraulic pressures less than the total pressure of the overburden.

These conclusions are compatible with field experience in fracturing and with the results of laboratory experimentation.

Discussion

Hubbert and Willis review the principles of stress distribution underground, the use of Mohr envelopes for analysis of fracture, laboratory sand-box and fracturing model experiments, and field evidence, as they apply to hydraulic fracturing. The bibliography cites a number of useful studies of fracturing.

Two quotations restate the premise for the present study: "... an understanding of the regional subsurface stresses makes it possible to analyze the stress conditions around the borehole and to determine the actual conditions under which hydraulic tension fractures will be formed," and "Present field data...are fully consistent with the foregoing conclusions" (predicted orientation of hydraulic fractures). Dike emplacement is much like artificial fracturing; the authors cite an analysis of the mechanical regime for emplacements at Spanish Peaks, Colorado.³² They note that many areas are in "relaxation" rather than active tectonism; accordingly, least stress is in the horizontal plane, and fractures are vertical. These should be mostly aseismic regions like most of the tight gas-sand area.

Other conclusions (not listed in the author's abstract):

- State of underground stress depends on tectonic conditions.
- Breakdown pressures are affected by preexisting regional stresses, hole geometry, and penetrating quality of the fluid.
- Minimum injection pressures depend "solely" on the magnitude of the least principal regional stress.
- In geologically simple and tectonically relaxed areas, fractures should be vertical, and in a single field they should have roughly the same strike.

Murray, G.H., Jr., "Quantitative Fracture Study—Sanish Pool, McKenzie County, North Dakota," *Am. Assoc. Pet. Geol. Bull.* **52**, 57-65 (reprinted in *Fracture-Controlled Production*, AAPG Reprint Series No. 21, AAPG, Tulsa, 1977).

Abstract

The Devonian Sanish pool of the Antelope field has several unusual characteristics which make it almost unique in the Williston Basin. Some of these are: (1) high productivity of several wells from a nebulous.

ill-defined reservoir; (2) association with the steepest dip in the central part of the basin; (3) very high initial reservoir pressure; and (4) almost complete absence of water production.

Analysis of these factors indicates that Sanish productivity is a function of tension fracturing associated with the relatively sharp Antelope structure. Fracture porosity and fracture permeability can be related mathematically to bed thickness and structural curvature (the second derivative of structure). It is found that fracture porosity varies directly as the product of bed thickness times curvature, and that fracture permeability varies as the third power of this product. A map of structural curvature in the Sanish pool shows good coincidence between areas of maximum curvature and areas of best productivity.

Volumetric considerations show that the quantities of oil being produced cannot be coming from the Sanish zone. It is concluded that the overlying, very petroliferous Bakken shale is the immediate, as well as the ultimate, source of this oil. The role of the Sanish fracture system is primarily that of a gathering system for many increments of production from the Bakken.

The extremely high initial reservoir pressure indicates that the Sanish-Bakken accumulation is in an isolated, completely oil-saturated reservoir and, hence, is independent of structure in the normal sense. Similar accumulations should be present anywhere in the Williston Basin where a permeable bed, of limited areal extent, is in direct contact with either of the two Bakken shale beds.

Discussion

Fracturing (as defined by well productivity) correlates well with mechanical theory using assumed rock tensile strengths. The fractures would conform to those shown by Stearns and Friedman²² for late intense deformation with maximum compressive stress parallel to the axis of folding.

No correlation is given to evaluate the calculated fracture porosity and permeability. Production history might be used now for calculating the permeability.

This work is often cited for the relation of fracturing to deformation. It is an example from the edge of the Rocky Mountain foreland.

Price, N.J., *Fault and Joint Development in Brittle and Semi-Brittle Rock* (Pergamon Press, London, 1966).

Introduction

Joints are cracks and fractures in rock along which there has been extremely little or no movement. They are the most commonly developed of all structures, since they are to be found in all competent rocks exposed at the surface. Yet, despite the fact that joints are so common and have been studied widely, they are perhaps the most difficult of all structures to analyze. The analytical difficulty is attendant upon a number of fundamental characteristics of these structures. Thus, there is abundant field evidence that demonstrates that joints may develop at practically all ages in the history of rocks. In sedimentary rocks, for example, joints may develop soon after deposition, while the sediments are still unconsolidated. They may possibly develop towards the end of a phase of active tectonic compression, and be associated with faults and folds. Or they may develop much later, when the phase of active deformation is not necessary to the development of joints. For competent rocks which exhibit no evidence of tectonic deformation are cut by joints.

In the light of these observations, it is unlikely in the extreme that all joints are the results of a single mechanism.

Another difficulty in joint analysis springs from the fact that, characteristically, joints exhibit little or no displacement along the joint plane. Consequently, except in special instances, it is extremely difficult, even impossible, to establish the age relationship of joint planes with one orientation to those with a different orientation. As a result, incorrect assumptions regarding the ages of joints may easily be made and this can invalidate the conclusions of the analysis.

Discussion

Price presents a comprehensive discussion of joints in Chapter 3, including classification, mechanical theory, laboratory and field data, and a comprehensive bibliography. His definitions and classification are objective without genetic connotation. He would prefer, however, to restrict the term "joint" to the result of brittle fracture and to distinguish it from other planar features and foliations that may be due to flow or ductile strain.

This book is also a comprehensive review of the literature to 1966; some of the citations are also reviewed elsewhere in this report.

Although Price emphasizes the multiple causes of joints, he points particularly to the changes in stress regime due to burial, uplift, and unloading, and how they promote jointing. They can be related to local stress conditions and local structures. There are several observations of parameters affecting joint frequency:

Joint and Fault Frequency. Joint frequency is many times greater than fault frequency (each joint relieves stress only in the immediate vicinity of a joint, while fault movement may relieve stress over a wide area.

Joint Frequency vs Lithology. Frequency appears related to the strain energy stored in a body of elastic rock, and is inversely proportional to Young's modulus of the rock. Therefore the "weaker" rock has more joints; e.g., coal, with joint spacing a fraction of an inch ($E = 2 \times 10^5$ psi) and sandstone, with joint separation of a foot or more ($E = 1 \times 10^7$ psi).

Joint Frequency vs Bed Thickness. Lithology being equal, frequency is inversely related to bed thickness. Analysis indicates this is due to frictional forces between adjacent beds.

Joint Frequency vs Degree of Tectonic Deformation. Normalized for lithology and bed thickness, joint frequency is directly related to structure curvature or rate of change of dip and strike. Harris, Taylor, and Walper²⁷ are cited. Murray²⁸ demonstrated this at the Sanish pool in North Dakota.

Price, N.J., "The Development of Stress Systems and Fracture Patterns in Undeformed Sediments," in *Proc., 3rd Congr. of the Int. Soc. for Rock Mechanics* (National Academy of Sciences, Washington, D.C., 1974), Vol. 1, pp. 487-496.

Abstract

In this paper the development of stress systems and fracture patterns in undeformed sediments are considered in relation to the accumulation of a sedimentary series, its downwarp and subsequent uplift and the concomitant de-watering of the sediments. It is indicated that high lateral stresses may develop in the rock at relatively shallow depths as a result of these processes. The fracture patterns predicted by this analysis are in excellent agreement with those observed in the field.

Discussion

Price emphasizes that joints can develop *without* tectonic processes other than downwarp and uplift. He shows the large stresses developed, and the importance of retained pore pressure in less permeable rocks that may on uplift cause tensile fracturing. He shows that systematic fractures in sets normal to each other, and with oblique shear sets, can develop in areas of little or no folding. Retained pore pressure during downwarp and uplift is important in the less permeable rocks, such as tight gas sands. Orientation of fractures appears to be related to basin dimensions or perhaps more fundamentally to direction of maximum rate of change of dip or bed curvature. (This is similar to the situation in more tightly folded rocks.)

Hodgson's¹⁵ appeal to earth tides and material fatigue is not required if this analysis is accepted.

Raleigh, C.B., "Crustal Stress and Global Tectonics," in *Proc. 3rd Congr. of the Int. Soc. for Rock Mechanics* (National Academy of Sciences, Washington, D.C., 1974), Vol. 1, pp. 593-599.

Summary

The earth's surface is divided into large plates of the crust and uppermost mantle which move relative to each other at a few centimeters per year. The boundaries of the plates are regions of intense tectonic activity where most earthquakes and currently active volcanoes are located. The driving mechanism for the plate motion is still poorly understood. Orientations of the stress fields at points within the plates may provide evidence as to the mechanism of plate motion. Compilations of earthquake focal mechanism solution and *in situ* stress measurements for the western United States show good agreement between the two. The Intermountain Seismic Belt and the Basin and Range provinces are regions of approximately E-W extension; the far western United States is in a state of right-lateral shear related to the boundary of the North American plate with the Pacific plate.

Discussion

Additionally, Raleigh's data include a tabulation of overcore and hydraulic fracture-derived directions of principal *in situ* stresses in the Uinta Basin. These correlate well with the major structures; e.g., Rangely anticline, some gilsonite dikes, and the Duchesne fault zone. Other data (i.e., southeast of Duchesne) might be interpreted if very young adjustments are postulated. These results suggest the possibility of predicting *in situ* stress and extrapolating measured stresses in areas of simple structure to aid in finding natural fracture production and in designing artificial fracture jobs.

Quite consistent earthquake focal plane solutions show that stress directions can be relatively uniform over large areas.

Raleigh is perplexed to explain the Uinta Basin results by plate tectonic theory since the area is in the interior of a continental plate. Either the stress is residual from the early Tertiary, as its coincidence with structure implies, or present plate-derived stresses are coincident with the earlier stresses. Raleigh prefers the latter explanation.

Focal plane solutions are obviously not available for the generally aseismic areas of the foreland basins where the tight gas sands are.

Stresses are shown as follows: maximum compressive stress in directions radial to the center of the Colorado Plateau, east-west to southeast in the Basin and Range, and north-south in the intermountain seismic belt (the over-thrust belt). This may imply present east-west extension (north-south maximum compressive stress) in much of the tight gas sand area.

Further *in situ* measurements will fill in the data for aseismic areas and may resolve the question of residual vs new stress systems.

Stearns, D.W. and M. Friedman, "Reservoirs in Fractured Rock," in *Stratigraphic Oil and Gas Fields*, Amer. Assoc. Pet. Geol. Memoir 16 (AAPG, Tulsa, 1972), pp. 82-106 (reprinted in *Fracture-Controlled Production*, AAPG Reprint Series No. 21, AAPG, Tulsa, 1977).

Abstract

In recent years three developments which have evolved more or less independently, when related, may be of value to the petroleum industry. First is the recognition, through normal oil field development, that fractures are significant to both reservoir capacity and performance. Second is the fact that controlled laboratory experiments have produced, in increasing quality and quantity, empirical data on rupture in sedimentary rocks. These data have been segregated to demonstrate the individual control on rupture of several important parameters: rock type, depth of burial, pore pressure, and temperature. The third development consists of the discovery of new methods to recognize, evaluate, use, and, in some cases, see fractures in the subsurface. This discussion of these three developments may help geologists and engineers to find new approaches to exploration and exploitation of fracture reservoirs. Reservoir and production engineers presently make the greatest use of fracture data, but geologists should find this information useful in exploration for oil and gas trapped in subsurface fractures. Except in the search for extensions to proved fracture reservoirs, there is in the literature a paucity of clear-cut examples of the use of fracture porosity data in advance of drilling.

For this reason, several speculative exploration methods discussed herein implement mapping of fracture facies as well as stratigraphic facies.

Discussion

Stearns and Friedman review the theoretical and experimental basis for fracturing, and the field evidence. They discuss measurement methods and review the relation of fractures to porosity and permeability.

Related to tight gas sands, they identify three types of fracturing: (1) fracturing related to faulting and caused by the same stress system, (2) a conjugate system mostly oriented in the dip direction in folded rocks formed during early or moderate folding, and (3) a system mostly perpendicular to dip in later or more severe folding. Type (2) and Type (3) fractures are normal to bedding; they change orientation with location on a fold. Price¹⁶ has also noted this relationship to bedding. Type (2), if confirmed, would be important in the subtle folds associated with many tight gas sand fields; e.g., Wamsutter Arch, Wyoming. The relation to long axes of sand bodies might be established. The writers point out the significance of the relative brittle behavior of rock types in exploring for structural zones; e.g., behaviors of shale vs dolomite or chert.

From their Summary and Conclusions:

"A basis for the prediction of the relative development and orientations of fractures in an unknown province is provided by an understanding of the interactions between three primary factors:

(1) The physical environment at the time of fracturing; i.e., effective confining pressure, temperature, and strain rate. These three parameters strongly affect the behavior of rock material.

(2) The magnitudes and orientations of the three principal stresses in the rock body at the time of fracture. The relative stress differences control the locations of the fractures, and the orientation of the stress field determines the potential fracture orientations.

(3) The nature of the sedimentary layer, including the degree of induration at the time of fracturing and the relative thickness of the rock units. Thickness and lithology determine which rocks in a mixed sequence are more likely to be fractured."

"Precise predictions of fracture spacing, areal extent, width, types (shear or extension), and exact locations within a rock body are not possible because the processes of fracturing and the compositions of the deformed body are so complex. It is possible to specify, at least approximately, the history of burial of a rock unit and something of its present structural geometry. From the former, the maximum temperature and overburden pressure affecting the rock can be determined. Qualitative predictions of the expected fracture development and orientation can be made from knowledge of the general geology, the known associations of fractures with structures, and the relations of fracturing to rock type, thickness, and structural position. Outcrop studies can be made initially and projected into the subsurface. As more seismic and well data become available, the prediction will become more quantitative. Though fracturing is a complicated process, laboratory and field studies provide as good a basis for estimating fracture development and trends as is available for many other geologic phenomena which are fearlessly predicted during the exploration of an area."

Voight, B., and B.H.P. St. Pierre, "Stress History and Rock Stress," in *Proc. 3rd Congr. of the Int. Soc. for Rock Mechanics* (National Academy of Sciences, Washington, D.C., 1974), Vol. 2, pp. 580-582.

Summary

We present an approach by which the "stress history" effect of gravitational, thermal, and tectonic stress components on the state of stress of a rock mass can be assessed in detail. Implications with respect to geotechnics and tectonophysics are significant.

In many cases it appears necessary to consider the complete *gravitational, thermal, and tectonic* loading history in detail, in order to ascertain those aspects of geological history which have left an imprint on existing force fields within the rock mass. The purpose of this paper is to suggest a method by which the important effects of stress history on the *in situ* stress state can be outlined.

Discussion

Voight and St. Pierre attempt a quantitative mathematical treatment of stress history and fracturing. They repeat the notion that fracturing occurs with unloading, whether due to "unflexing" of strata with uplift or due to denudation. In this, they support the ideas of Price.²⁴ Microfracturing may relieve compressive stresses, but if fractures are few, or if they are filled with cementing material, compressive stresses may develop. These are relieved by exfoliation-type fractures parallel to the free surface; e.g., in Appalachian granites.

A measurement of residual stress direction might be developed from the authors' observation: "The statistical maximum of available compressive strain energy is oriented perpendicular to the statistical maxima of microfracture trends; thus, maximum compression induced from this mechanism can be predicted from observed microfracture fabric."